Diagenesis and Stratigraphy of the Lisburne Group Limestones of the Sadlerochit Mountains and Adjacent Areas, Northeastern Alaska

GEOLOGICAL SURVEY PROFESSIONAL PAPER 857

DIAGENESIS AND STRATIGRAPHY OF THE LISBURNE GROUP LIMESTONES OF THE SADLEROCHIT MOUNTAINS AND ADJACENT AREAS, NORTHEASTERN ALASKA

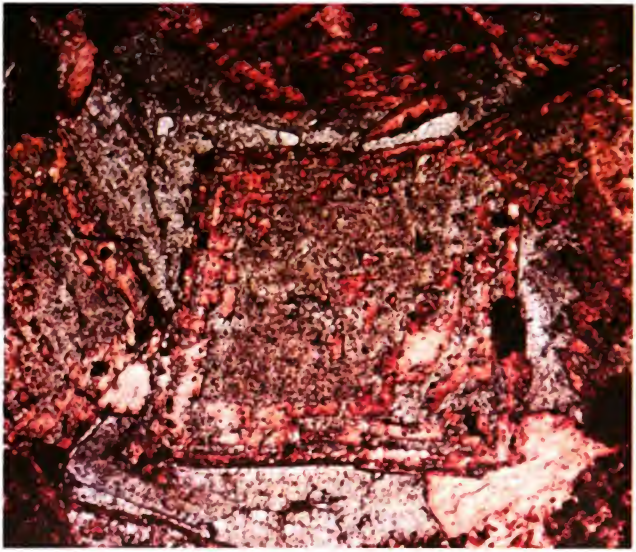

Rhombs of dolomite set in sparry calcite. The red-stained zones parallel to the original rhomb faces are calcite (dedolomite). Overgrowths of homogeneous dolomite occur in two stages parallel to the lines of intersection of the rhomb faces. Patches of hematite (black) developed at the edge of the original rhomb and are included within the overgrowth; others developed on the outer edge of the overgrowths. Plane-polarized light. Stained by Alizarin Red S.

Diagenesis and Stratigraphy of the Lisburne Group Limestones of the Sadlerochit Mountains and Adjacent Areas, Northeastern Alaska

By GEORGE V. WOOD and AUGUSTUS K. ARMSTRONG

GEOLOGICAL SURVEY PROFESSIONAL PAPER 857

Biostratigraphy and depositional environments of the Lisburne Group, with a detailed account of the relative age of diagenetic events affecting the carbonate rocks and an analysis of the resultant mineralogical changes

UNITED STATES GOVERNMENT PRINTING OFFICE, WASHINGTON : 1975

UNITED STATES DEPARTMENT OF THE INTERIOR

ROGERS C. B. MORTON, *Secretary*

GEOLOGICAL SURVEY

V. E. McKelvey, *Director*

Library of Congress Cataloging in Publication Data

Wood, George V.
Diagenesis and stratigraphy of the Lisburne Group limestones of the Sadlerochit Mountains and adjacent areas, northeastern Alaska.

(Geological Survey Professional Paper 857)
Bibliography: p. 38.
Includes index.
Supt. of Docs. No.: I 19.16:857
1. Limestone–Alaska–Sadlerochit Mountains. 2. Diagenesis–Alaska–Sadlerochit Mountains. 3. Geology, Stratigraphic–Carboniferous. 4. Geology–Alaska–Sadlerochit Mountains. I. Armstrong, Augustus K., joint author. II. Title. III. United States. Geological Survey. Professional Paper 857.
QE471.15.L5W66 552'.5 74-26965

For sale by the Superintendent of Documents, U.S. Government Printing Office
Washington, D.C. 20402 - Price $2.25 (paper cover)
Stock Number 024-001-02658-9
Catalog Number I19.16:857

CONTENTS

ILLUSTRATIONS

[Plates follow index]

TABLES

DIAGENESIS AND STRATIGRAPHY OF THE LISBURNE GROUP LIMESTONES OF THE SADLEROCHIT MOUNTAINS AND ADJACENT AREAS, NORTHEASTERN ALASKA

By GEORGE V. WOOD[1] and AUGUSTUS K. ARMSTRONG

ABSTRACT

Four complete sections of the Mississippian and Pennsylvanian limestones of the Lisburne Group in or adjacent to the Sadlerochit Mountains were sampled at 5- to 10-foot intervals for petrographic study. The Sadlerochit Mountains are shown to have been a landmass during Meramecian time and to have been subsequently submerged during the Chesterian transgression (Zone 16). Regional transgressions also occurred during Meramecian time (Zone 13) and at the beginning of Pennsylvanian (Zone 20) time.

The Alapah Limestone (Mississippian) has a dominantly lime-mud matrix and in many places is dolomitized toward the top, whereas the Wahoo Limestone (Pennsylvanian) is dominantly a grainstone facies with intergranular sparry calcite. The grains of the limestones are mostly crinoids, bryozoans, and pelecypods, together with pellets and oolites. The depositional environment ranged from supratidal to subtidal. The genesis of the oolite grains is discussed in particular detail, and it is concluded from recent work on the amino acid content that biochemical elements have a large influence on their origin.

Two phases of sparry calcite cementation occurred in the grainstone facies; the first phase is a fringe around the clasts and is free of iron, and the second phase fills the remaining intergranular spaces and is commonly rich in iron. The dolomites are considered to be of early diagenetic origin. The coarse dolomite rhombs that occur as accessories in the grainstones are rich in iron and tend to be zoned. These rhombs are prone to dedolomitization. The dedolomitization process is not of recent origin, as demonstrated by postdedolomitization overgrowths of iron-free dolomite. It is more likely to have occurred during a period of emergence during Chesterian time.

Two types of chert are distinguished: "matrix" chert and intragranular chert. The "matrix" chert is considered to be of direct biogenic origin. The intragranular chert, usually restricted to the grainstone facies, formed within pelecypod shells or crinoid plates by the reaction of silica in the sea water with the organic tissue in the bioclast to form a short-lived organosilicic acid. This acid, in turn, reacted with the calcite of the bioclast to precipitate silica on a piecemeal basis.

Anhydrite, celestite, and barite have been identified in the Lisburne Group limestones of the subsurface, and their association with algal mats suggests that sabkha-type sedimentation of the present-day Arabian Gulf is a depositional model for these beds. Marble interbedded with unaltered sedimentary limestones in the western Sadlerochit Mountains is considered to be a product of dynamic metamorphism restricted to the sole of a major thrust plate.

The fabrics common in the limestones of the Old Man Creek section are attributed to thermal alteration related to the intrusion of the Mount Michelson pluton; the pluton, in turn, suggests that the granite is post-Pennsylvanian in age.

Diagenetic modification of the Lisburne Group limestones was nearly complete before the marbles, stylolites, and calcite-filled fractures formed. The rock fabrics remain virtually the same today.

INTRODUCTION

The four outcrop sections of carbonate rocks from the Sadlerochit Mountains and adjacent areas of the northeastern Brooks Range (fig. 1) represent most of the typical rock types and environments of deposition of the Lisburne Group. We believe a study of the history of sedimentation and diagenetic processes of these sections will be applicable to most other outcrops of the Lisburne Group in the Brooks Range and in the subsurface of the North Slope. A detailed study of the sedimentation and diagenesis gives one insight into the complex geologic history of the Lisburne Group and facilitates the construction of lithofacies maps. The knowledge gained from this study is readily applicable in helping to predict the porosity trends in the Lisburne Group of the subsurface.

PREVIOUS WORK

Schrader (1902) was the first to apply the name Lisburne Formation to the carbonate rocks at Anaktuvuk River valley, which were incorrectly dated as Devonian. Later studies (Collier, 1906, p. 22–26) revealed the limestones to be Mississippian in age. In the Shainin Lake area (fig. 1), Bowsher and Dutro (1957, p. 3, 4, 6) recognized two new formations within the Lisburne, which they raised to group rank. The lower formation, the Wachsmuth Limestone, is divided into four informal members and overlies the Kayak Shale. The upper formation, Alapah Limestone, overlies the Wachsmuth Limestone and has nine informal members. The Alapah Limestone at its type locality is covered by Pleistocene glacial gravel and alluvium.

[1]British Petroleum Co., Ltd., BP Research Centre, Chertsey Road, Sunbury-on-Thames, Middlesex, England.

FIGURE 1.—Map of arctic Alaska showing location of the area studied, outcrop pattern of Carboniferous rocks, and significant oil exploration stratigraphic test wells.

Brosgé, Dutro, Mangus, and Reiser (1962) described the Paleozoic sequence in the eastern Brooks Range. In this region they recognized three formations within the Lisburne Group: the Wachsmuth and Alapah Limestones and an overlying limestone that they named the Wahoo Limestone. They assigned the Wahoo a Pennsylvanian(?) and Permian age.

Armstrong, Mamet, and Dutro (1970) and Mamet and Armstrong (1972) reported the Lisburne Group within the area of this study to be of Late Mississippian to Middle Pennsylvanian (Atokan) age. The age assignments are based on microfossil assemblages. The coral fauna, biostratigraphy, and paleoecology of the Wahoo Limestone in the Sadlerochit Mountains was described by Armstrong (1973).

Petrographic studies of the carbonate rocks of the Lisburne in the Endicott Mountains, central Brooks Range, were made by Krynine, Folk, and Rosenfeld (1950) for the dolomites and Krynine and Folk (1950) for the limestones. Armstrong (1970b) published a short report on the petrography of Mississippian chert and dolomites from the Lisburne Group in the Killik River–Mount Bupto Region, Brooks Range.

ACKNOWLEDGMENTS

The fieldwork for this study was done by Armstrong. We wish to express our appreciation to I. L. Tailleur, the party chief, summer of 1968, and H. N. Reiser, the party chief, summers of 1969 and 1970, for their generosity in supporting the stratigraphic studies. We also thank the Naval Arctic Research Laboratory (Barrow), Office of Naval Research, for their logistical support of fieldwork in the summers of 1968, 1969, and 1970.

George Wood is responsible for the petrographic work and diagenetic history. We thank the Chairman of the British Petroleum Co., Ltd., for permission to carry out this study and to publish its conclusions. Dr. P. E. Kent, F.R.S., Assistant General Manager, Exploration, and Wood's colleagues at the British Petroleum Research Centre have given considerable encouragement to the work. Dr. R. Walls and Mrs. E. Aston, in particular, are thanked for their help in interpreting the metamorphic fabrics. Professor B. L. Mamet of the Université de Montréal determined the foraminiferal zones in the stratigraphic sections.

STUDY METHOD

This study is based on measured stratigraphic sections from which lithologic and foraminiferal samples were collected at intervals of 5–10 feet. Thin sections were cut from the samples to determine the microfossil assemblages and the carbonate petrography and microfacies. Dr. B. L. Mamet identified the microfossils, and his microfossil zones are the basis for the regional stratigraphic correlations in this study. Detailed documentation of the microfossil zones used in the

stratigraphic section of this report can be found in Armstrong, Mamet, and Dutro (1970) and Mamet and Armstrong (1972).

The carbonate rock classification used in this report is that of Dunham (1962) (table 1). The lithologic and paleontologic symbols used in this report are shown in figure 2.

DESCRIPTION OF SECTIONS

The four sections described in detail in this paper (fig. 2), Plunge Creek, 70A–4/5; western Sadlerochit Mountains, 69A–1; eastern Sadlerochit Mountains, 68A–4A/4B; and Old Man Creek, 69A–4/4K, were sampled at 5- to 10-foot intervals. The detailed petrography, largely done by Wood, is based on thin-section study of these samples and is integrated with the field descriptions by Armstrong. The overall percentage of major rock types in three of the sections is given in table 2; the Old Man Creek section has been omitted because sporadic intense recrystallization has obliterated a large part of the original fabric.

In general, there is a progressive west-east increase in the proportion of grainstone, and a related west-east decrease in the proportion of mud-supported carbonates (that is, wackestone and mudstone). The proportion of dolomite has a strong maximum in the Plunge Creek section, but it must be pointed out that the proportion of dolomite in Old Man Creek (42 percent) is even higher. Between 14 and 20 percent of the limestone in the three sections is dolomitic.

The sections are subdivided into units on the basis of their dominant lithologic characters, but some of the subdivisions are rather arbitrary because of the mixing of rock types. The depths referred to are those of the total thickness of the Lisburne Group taken from the base of the section and recorded on the right of the stratigraphic columns in figure 2.

TABLE 2.—*Percentage of major rock types in the Lisburne Group in three sections*

Rock type	70A–4/5 Plunge Creek section[1]	69A–1 Western Sadlerochit Mountains section[2]	68A–4A/4B Eastern Sadlerochit Mountains section[3]
Grainstone	21	47	55
Packstone	26	33	24
Wackestone/mudstone	12	11	6
Dolomite	33	9	15

[1]7 percent is chert. 15 percent of limestone is dolomitic
[2]15 percent of limestone is dolomitic
[3]14 percent of limestone is dolomitic.

70A–4/5, PLUNGE CREEK

The base of the Lisburne Group in the Plunge Creek section is taken arbitrarily where the carbonate content becomes dominant over the shale of the underlying Kayak(?) Shale. The Kayak(?) Shale is 1,290 feet thick and it rests on 30 feet of the Kekiktuk Conglomerate, which in turn rests unconformably on tilted Neruokpuk Formation.

The basal unit (0–330 ft) of the Lisburne Group in this section is argillaceous and dolomitic wackestone and mudstone. The rock represents a continuation of the quiet open-water marine sedimentation that persisted during the deposition of the Kayak(?) Shale but differs by being dominated by carbonate. Foraminifera and finely comminuted crinoid debris are the dominant faunal elements. The interrhombic spaces in the macrodolomites that commonly occur within this unit are filled with dark clay minerals, the residue after completion of the dolomitization process. From 330 to 720 feet is a homogeneous unit composed mostly of macrodolomite in which the rhombs are larger than 50 micrometres.

In the interval 550–558 feet, which may be correlative with the interval 50–65 feet in the western Sadlerochit Mountains section (69A–1), the dolomite

TABLE 1.—*Classification of carbonate rocks according to depositional texture (Dunham, 1962, p. 117)*

Depositional texture recognizable					Depositional texture not recognizable
Original components not bound together during deposition				Original components were bound together during deposition*** as shown by intergrown skeletal matter, lamination contrary to gravity, or sediment-floored cavities that are roofed over by organic or questionably organic matter and are too large to be interstices.	*Crystalline carbonate*
Contains mud (particles of clay and fine silt size)			Lacks mud and is grain-supported		
Mud-supported		Grain-supported			
Less than 10 percent grains	More than 10 percent grains				(Subdivide according to classifications designed to bear on physical texture or diagenesis.)
Mudstone	*Wackestone*	*Packstone*	*Grainstone*	*Boundstone*	

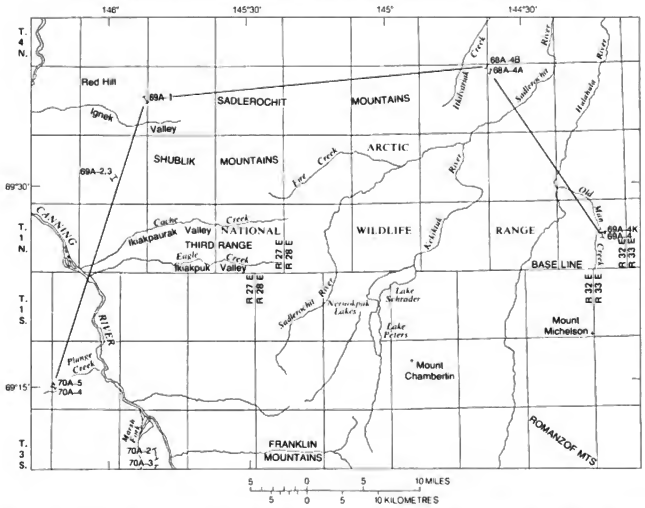

FIGURE 2.—Correlation diagram for the Lisburne Group in the Sadlerochit Mountains and adjacent areas. Biostratigraphic zonation is based on the microfossil zones of B. L. Mamet. Index map showing location of the stratigraphic sections and symbols used for fossils and lithology is shown on the lower part of this diagram. The cross section for 70A-2 and 70A-3 is in figure 12.

rhombs are etched and partly replaced by sparry calcite (dedolomitized).

From 720 to 918 feet (fig. 3) is a sequence of diverse rock types ranging from crinoid bryozoan grainstone to packstone with intervals of macrodolomite. Pellets and oolites also occur sporadically. The depositional environment probably was marginal between the area of shoal-carbonate deposition and the open platform. The intervals of macrodolomite contain evidence of two generations of dolomite formation. The zoned first-phase dolomites, sometimes in rich iron, are crosscut both by iron-poor second-phase dolomite and by sparry calcite cement.

Above 918 feet is a unit of dolomitic wackestone and packstone with crinoid and bryozoan debris (to 1,190 ft). Macrodolomite is predominant over the basal 50 feet. Matrix chert is common, particularly in the upper 65 feet. The chert contains as much as 40 percent of macro- and micro-dolomite, often with individual rhombs intensely corroded. The presence of ghosts after sponge spicules suggests that the chert is of direct biogenic origin.

In the interval 1,190–1,630 feet macrodolomite is the dominant rock type and is regularly intercalated with dolomitic bryozoan crinoid wackestone and packstone. Except for the change in the relative abundance of mac-

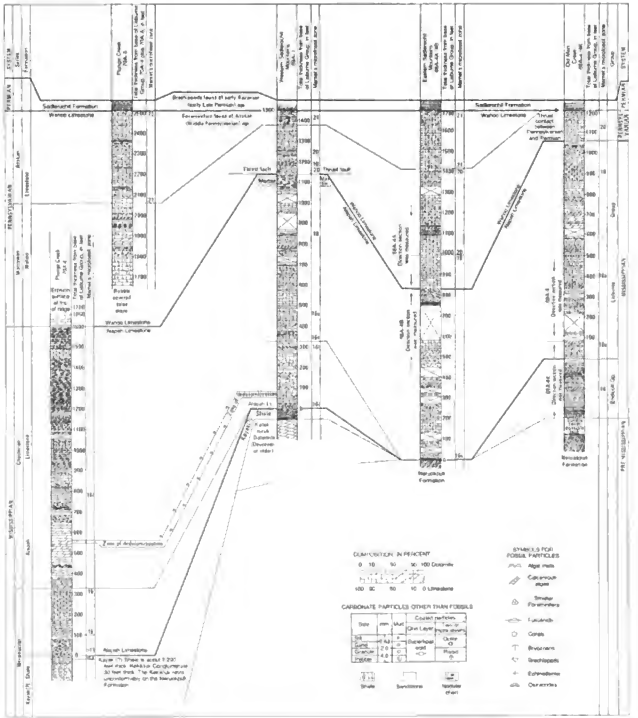

FIGURE 2.—Continued.

FIGURE 3.—Alapah Limestone at Plunge Creek sections 70A–4-5. Line of traverse shown by arrows along crest of ridge.

rodolomite, this interval is markedly similar to the lower unit (918–1,190 ft). Matrix chert is again common with microdolomite rhombs and ghosts after sponge spicules. Dolomite rhombs in the macrodolomite are commonly outlined by iron oxide. Crinoid debris in these rocks commonly has bent twin planes suggesting at least two phases of earth movement.

From 1,630 to 1,880 feet the rock is uniform bryozoan crinoid packstone containing as much as 30 percent intergranular dolomite in the carbonate mud. The upper 55 feet is macrodolomite with remains of bryozoan debris still preserved in calcite. The depositional environment of this unit was probably an open-water platform beyond the zone of water agitation, but the occurrence at 1,880 feet of polycrystalline quartz preserved with the external morphology of an anhydrite nodule suggests that the macrodolomite in the interval 1,825–1,880 feet may have been deposited in an intratidal/supratidal environment.

Above 1,800 feet (fig. 4), and persisting to the top of the section at 2,505 feet, is a homogeneous unit of grainstone in which all the intergranular space is occupied by sparry calcite cement.

Coarse-grained bryozoan and crinoid debris is the dominant clastic element, but sporadic intervals of oolites or pellets also occur. Intragranular chert is commonly nucleated within crinoid plates, in contrast to the dominant matrix chert in the interval 918–1,630 feet. The depositional environment of this unit was probably shoals of bioclastic debris from which all available carbonate mud had been winnowed.

69A–1, WESTERN SADLEROCHIT MOUNTAINS

The lowermost 50 feet of this section, which consists of shales with limestone lenses, has been questionably assigned to the Kayak Shale unconformably overlying the tilted Katakturuk Dolomite of Devonian or older age.

The lowermost limestone unit (0–65 ft), which consists of wackestone and packstone with fine-grained bioclastic debris dominated by crinoids, appears to be a continuation of the sedimentary pattern of the Kayak(?) Shale but with an almost total absence of clay minerals.

The upper part of this unit is characterized by extensive early dedolomitization that may be evidence of emergence; this is discussed in detail in the section on diagenesis. From 65 to 470 feet the rock is largely sporadically dolomitized, medium-grained, bryozoan, crinoid, and pellet grainstone with scattered oolitic layers. The rock types reflect a shallowing of the water, suggesting that water agitation was sufficient to remove the bulk of the available carbonate mud to a quieter area. The environment was probably a shallow marine shelf with clumps of bryozoans and crinoids. Abundant fecal pellets suggest that the patches of car-

FIGURE 4.—Plunge Creek section 70A–4/5. Footage is marked, as is the contact with the overlying Sadlerochit Formation. Photograph taken from helicopter; view north.

bonate mud were subject to considerable bioturbation. The overlying rocks (470–770 ft) are dominantly pellet bryozoan packstone with scattered thin dolomite beds; three intervals contain as much as 20 percent fine-grained quartz. The dolomite rhombs, as at 593 feet, commonly have an iron-rich core and an iron-free rim outlined in iron oxide. These rocks suggest a gradual reduction in the intensity of wave agitation, probably in an environment protected from waves with restricted access to open water and with intense bioturbation.

From 770 to 1,070 feet wackestones become more abundant, although packstones are still common. Bryozoan debris and pellets are the dominant grains. There are sporadic dolomites, and a large proportion of the intergranular carbonate mud contains dolomite rhombs that are commonly outlined by iron oxides. In the lower part of this interval, the original dolomite rhomb outlines are preserved, but the centers are commonly void. This interval represents a continuation of the protected environment suggested for the unit at 470–770 feet but with an increase in salinity.

At 1,070 feet there is a major change in rock type. Mineralogically, the rock is still calcite, but the original texture and nature of the grains have been obliterated by extensive metamorphic recrystallization that produced interpenetrating crystals. This rock must be referred to as marble and is almost certainly a product of metamorphism along a thrust plane at 1,140 feet in the section. This probable plane of dislocation coincides with the top of a marked break of slope, and the upper limit of the marble coincides with the suggested base of the Wahoo Limestone at 1,140 feet (fig. 5). The metamorphism is restricted to the sole of the postulated thrust with the intensity decreasing downward. It is not known how much of the original section is repeated or missing as a result of this suggested structural discontinuity. The details of the metamorphic fabrics are described in the section on "Diagenesis."

The basal rocks (1,140–1,325 ft) of the Wahoo Limestone are medium-grained bryozoan crinoid wackestone and packstones similar in type and depositional environment to the uppermost rocks of the Alapah Limestone (that is, from 770–1,070 ft), except that dolomite is almost totally absent. The uppermost rocks of the Wahoo Limestone are coarse-grained bryozoan crinoid

FIGURE 5.—Section 69A-1, western Sadlerochit Mountains, showing stratigraphic footages and contacts between Kayak(?) Shale, Alapah Limestone, Wahoo Limestone, and Sadlerochit Formation. Zone of metamorphic marble and thrust fault are also shown. View south.

grainstones (1,325–1,450 ft) with a 45-foot-thick oolitic grainstone interval near the top of the section. This unit represents a strongly agitated open-shoal environment with banks of oolites. Any carbonate mud that may have been present has been winnowed from the place of deposition, and the debris is extremely well sorted.

68A-4B, SUNSET PASS, EASTERN SADLEROCHIT MOUNTAINS

The basal 7 feet of this section immediately overlying tilted shales and sandstones of the Neruokpuk Formation consists of very coarse angular grains of quartz and chert cemented by sparry calcite. Hematite-rich clay laminae and size grading emphasize the layering. These rocks grade upward into pellet crinoid grainstones (0–360 ft) with scattered layers of packstones and mudstone. Matrix chert (section on "Chert") is common. The fact that carbonate mud is scattered throughout the grainstone suggests that the dominant depositional environment was an open platform close to the lower limit of wave agitation. Above 360 feet (up to 820 ft) the dominant rock type is macrodolomite with an intermediate interval of partly dolomitic grainstone (fig. 6). Individual dolomite crystals are clear, anhedral, and commonly about 50 micrometres in size. Interrhombic chert and calcite are common. The preferential development of dolomite in fine-grained carbonate rock suggests that the original rock in this interval contained a high proportion of carbonate mud. Algal-mat sediments were recorded at 760 feet in this section by Armstrong and this fact suggests that the dominant environment was intertidal to supratidal (Wood and Wolfe, 1969).

From 820 to 1,332 feet the dominant rock type is partly dolomitized fine- to medium-grained grainstone with subordinate packstones. Bryozoans and crinoids are the dominant clastic elements in the lower part of this unit, which contains pellets in the upper 240 feet. At 1,130 feet, fine quartz grains are a common accessory. Intragranular chert developed within crinoid plates is common. The dominant environment is an open marine shelf with the pellets representing the products of bioturbation of carbonate mud. The base of this interval (820 ft) is taken as the base of the Wahoo

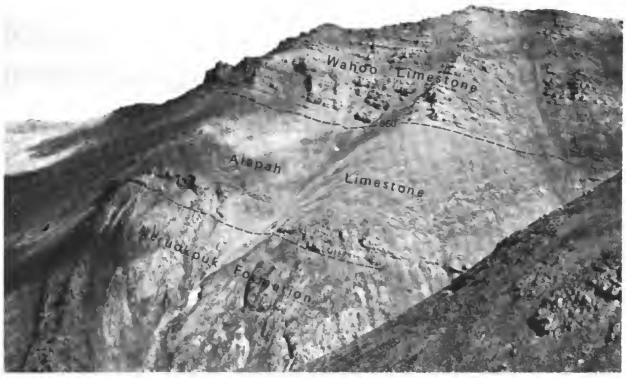

FIGURE 6.—Outcrop of the Lisburne Group on hillside east and opposite the line of traverse of eastern Sadlerochit Mountains sections 68A–4A/4B. Thin-bedded dolomite near the top of the Alapah Limestone forms the rubble-covered slope beneath the massive cliffs of Wahoo Limestone. The topographic expression of the Lisburne Group clearly reflects the different depositional environments in which the carbonate rocks formed. The Alapah Limestone is 830 feet thick.

Limestone. The second-stage sparry calcite cement (see section on "Sparry Calcite Cement") of this interval is very rich in iron.

From 1,332 to 1,562 feet the rock is mostly oolitic grainstone with rare oolitic packstones. The individual oolites have well-developed cores of either bryozoan or crinoid debris with four to five thin oolitic layers. The oolites tend to be of medium to coarse sand size and are well sorted. This rock type was probably deposited on an open-water marine bank, as shoals and dunes, in which intense water agitation was of sufficient strength to roll the bioclastic debris and allow concentric deposition of aragonite. The cores of these oolites range in shape from elongate to equidimensional, but it was obviously easier for oolite skins to develop on equidimensional cores. Elongate grains with oolitic skins can be considered an index of extreme water agitation. The rare oolite packstones probably resulted from incorporation of oolites of the banks into the adjacent and protected intershoal carbonate mud. Chert is commonly developed within crinoid plates, and the rare intergranular dolomite rhombs are edged with iron oxide. A slight modification of this oolitic horizon persists for 90 feet (1,562–1,652 ft); the bioclastic debris tends to be coated by the crenulated encrusting algae *Osagia* rather than by oolitic layers. The depositional environment was probably very similar to that of the underlying oolitic grainstones (Henbest, 1968).

From 1,652 to 1,692 feet at the top of the section the facies changes abruptly to pellet wackestone and packstone that is sporadically rich in both pyrite and sponge spicules. This rock type suggests a change in environment to a restricted platform protected from the main oceanic circulation. This kind of environment accounts for a high reduction potential.

69A–4/4K, OLD MAN CREEK

The Old Man Creek section is anomalous with regard to both thickness and facies because of intense tectonic and probable thermal metamorphic effects. The section is only about 7 miles north of the Mount Michelson pluton of Mount Michelson. Sheared greenstones and

pyroclastic rocks that crop out in Old Man Creek are considered (Reiser, 1970) to be pre-Mississippian in age. In the section on "Diagenesis," the case for a post-Pennsylvanian age of the Mount Michelson pluton is argued on the basis of the grain fabrics of the Lisburne Group in Old Man Creek, some of which are attributed to thermal metamorphic effects. The boundary between the Lisburne Group and the overlying Sadlerochit Formation is almost certainly a thrust fault as shown by the strongly sheared fabric (see pl. 6, figs. 3, 4).

The basal 290 feet of the section, probably separated from the Neruokpuk Formation by a fault, has been assigned to the Kayak(?) Shale of the Endicott Group, but the basal 210 feet contains completely recrystallized marble with annealed fabrics, argillaceous laminae, and unaltered macrodolomites. If the argument for the thrust origin of the marble unit of section 69A–1 (western Sadlerochit Mountains) holds, then this basal unit could well contain a series of thrust slices. The macrodolomites of this interval show no textural response to this suggested thrusting, but it is not necessary to postulate a posttectonic origin for the dolomite. As discussed in the section on "Marble," dolomite has a higher fracture point and greater ductility than calcite, which allows calcite to fracture (and anneal) while dolomite is still in the elastic field.

From the base of the Lisburne Group to 125 feet microdolomite is the dominant rock type with intercalated intervals of unfossiliferous lime mudstone. These rocks may represent syngenetic dolomitization of lagoonal carbonate muds.

Above 125 feet to 830 feet is a mixed association of dolomitic pellet packstone and grainstone with a high proportion of interbedded macrodolomite. Commonly, the macrodolomite crystals (sometimes edged with iron oxide) are replaced by sparry calcite as a result of marginal corrosion and spotty replacement within the crystals. This partial dedolomitization is probably a response to thermal metamorphism; this type of metamorphism is also emphasized throughout this interval by intense interfingering of the grain margins in the limestones.

From 830 to 930 feet is a thin interval of nondolomitic fine-grained crinoid wackestone with scattered fine quartz grains. An open-marine platform is the most likely environment for this interval.

From 940 to 1,032 feet is a homogeneous interval of microdolomite with several calcite-filled veinlets. These rocks are commonly layered as a result of ferruginous intergranular material that may represent original algal-mat laminations.

Above 1,060 feet to the top of the section, the rock assigned to the Wahoo Limestone probably was dominantly an original crinoid grainstone. Grain twinning and interpenetration are ubiquitous and tend to obscure the original fabric. Dedolomitized rhombs edged with iron oxide are common. In scattered horizons the formation of annealed calcite, probably along minor thrust planes, has totally obliterated evidence of the original rock type.

ENVIRONMENTS OF DEPOSITION

Depositional environments of the Lisburne Group (fig. 7) ranged from an openwater platform to shallow-water lime-sand shoals to areas of open and restricted platform with gradual increase in salinity related to partial separation from open marine circulation. This sequence terminated with the intertidal-supratidal environment in which algal mats are a characteristic feature. The representation of figure 7 in no way characterizes a particular time interval.

Figure 8 is an interpretation of the variation in depositional environment of the four stratigraphic sections described in the previous section. Decisions regarding the assignment of a particular rock type to a specific depositional environment were somewhat arbitrary, especially for the dolomites. If, for example, algal mats were observed in the field, an intertidal environment is inferred, but in the absence of other evidence, a restricted platform environment is indicated for dolomite units. The Alapah Limestone-Kayak(?) Shale boundary in section 70A–4/5 (Plunge Creek) occurs in Zone 13 of the Meramecian Series of the Upper Mississippian. The base of the two sections in the Sadlerochit Mountains is in Zone 16 (Chesterian Series); there it unconformably overlies Devonian or older rocks. Zone 14 is present in the Old Man Creek section. This variation in the nature and age of the base of the Alapah Limestone suggests that the Plunge Creek section lies in an area of constant downwarp, subsequent to the transgression of the Kayak(?) Shale which occurred probably during Meramecian time (< Zone 13). This Meramecian transgression is also recorded in the Ikiakpuk section (68A–1) (see fig. 2 for location). During Meramecian time the Sadlerochit Mountains was an area of nondeposition; it was probably a land mass exposing both the Katakturuk Dolomite of Devonian or older age and sandstone and shales of the Neruokpuk Formation. A second transgression submerged the Sadlerochit high during Zone 16 of the Chesterian Series of Upper Mississippian. This transgression was probably gradual; it flooded the western Sadlerochit Mountains during the early part of Zone 16 and completely submerged the high during the later part of Zone 16. The Old Man Creek area probably was also submerged by the Meramecian transgression.

Possible correlation lines (based on microfossil zones) between the four sections are illustrated in figure 2.

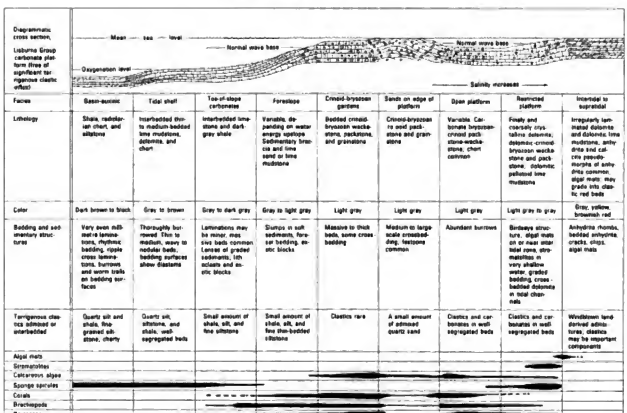

FIGURE 7.—Generalized depositional environments of the Lisburne Group, north flank, eastern Brooks Range.

During Zone 16 time in the three more westerly sections, open-platform sedimentation was dominant, although shoals of oolites and bioclasts were characteristic in the western Sadlerochit Mountains. Horizons of marked dedolomitization at 550 feet in the Plunge Creek section and 65 feet in the western Sadlerochit Mountains during Zone 16i suggest that uplift could have brought the rocks within a zone of fresh water at this time. It is possible that more landward conditions (restricted platform or intertidal) persisted in the Old Man Creek area. Later in the Chesterian (post-Zone 16) a marked regional regression occurred as suggested by the persistence of a restricted platform environment at the top of the Alapah Limestone. This shallowing went as far as intertidal conditions in the eastern Sadlerochit Mountains and Old Man Creek.

The third regional transgression traceable in the Sadlerochit Mountains occurred at about the boundary of the Alapah and Wahoo Limestones. This transgression is indicated by the abrupt change from a restricted platform environment of the upper Alapah Limestone to an open platform-shoal environment of the lower Wahoo Limestone (Armstrong, 1973). Although figure 8 shows that the plane of this transgression is not coincident with the boundary between the two formations, it must be remembered that this boundary was chosen in the field on the basis of a change of slope rather than on strictly lithologic characters. The plane of this Pennsylvanian (Morrowan) transgression probably approximates isochroneity better than the somewhat arbitrary boundary between these two limestone formations. The rocks deposited during the Morrowan (Zone 20) were open-platform grainstone and packstones throughout the area, but at about the Morrowan-Atokan boundary there was a probable regression, and shoal carbonate rocks (grainstones) became the dominant rock type. Oolitic grainstones are common in the eastern Sadlerochit Mountains, whereas ordinary bioclastic grainstones are dominant in the other sections. As in the other parts of the sections, the intergranular space of the grainstones has been completely obliterated by sparry calcite cement.

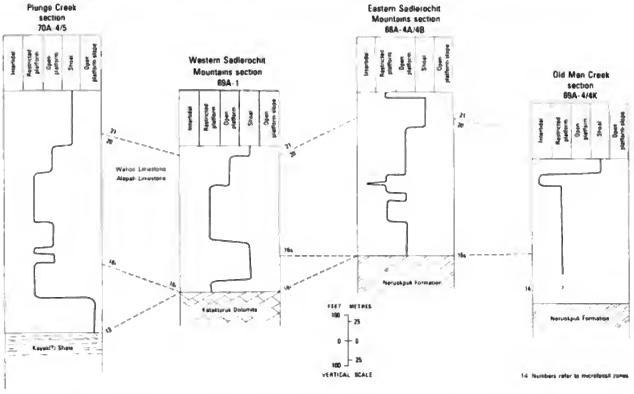

FIGURE 8.—Idealized graphs showing variation of depositional environments in the four stratigraphic sections.

BIOSTRATIGRAPHIC CORRELATION

Detailed discussions and faunal lists for the biostratigraphy of the Lisburne Group in the northeastern Brooks Range have been previously published, and these discussions and faunal lists are not repeated in this report.

The regional correlation chart (fig. 2) for the Lisburne Group and the correlation diagram for the sections discussed in this report (fig. 9) are based on B. L. Mamet's microfossil zones. Lists of the microfossils for the eastern Sadlerochit Mountains section 68A–4A/4B were published by Armstrong, Mamet, and Dutro (1970) and for the Plunge Creek 70A–4/5 and western Sadlerochit Mountains 69A–1 sections by Mamet and Armstrong (1972). The Old Man Creek (69A–4/4K) section has been zoned by Mamet, and the microfossil lists are in manuscript. Microfossils have proved to be the most reliable and efficient means of correlation within the Lisburne Group and with the standard American and Eurasian type sections.

The most conspicuous megafossils on the outcrop are rugose corals. Armstrong (1970a, 1972) analyzed the stratigraphic range of the lithostrotionoid corals and described parts of the fauna. He also (1973) described Wahoo Limestone corals of Atokan age, their paleoecology, and their regional distribution. In the Lisburne Group, corals are relatively abundant in Meramecian and Atokan age beds but scarce in Osagean and Chesterian beds. Their stratigraphic range is generally longer than individual microfossil zones; individual species of corals generally range through three or more microfossil zones.

Mamet and Armstrong (1972) reported that at the Plunge Creek section the Kekiktuk Conglomerate, which directly overlies the Neruokpuk Formation, is about 25 feet thick and is overlain by 1,295 feet of shales and argillaceous limestones of the Kayak (?) Shale. Mamet and Armstrong (1972) described a microfauna and corals of Zone 11, Meramecian, in the Kayak (?) Shale about 550 feet above the Neruokpuk. As shown in figure 2, the Kayak (?) Shale is thin in the Sadlerochit Mountains, only about 50 feet thick in the western Sadlerochit Mountains section, and absent from the eastern Sadlerochit Mountains section. There the Alapah Limestone of Chesterian age rests directly on the Neruokpuk Formation. In the Old Man Creek section to the southeast, the Kayak(?) Shale contains lithostrotionoid corals and microfossils of Zone 14, Meramecian, and is at least 300 feet thick. Here exact

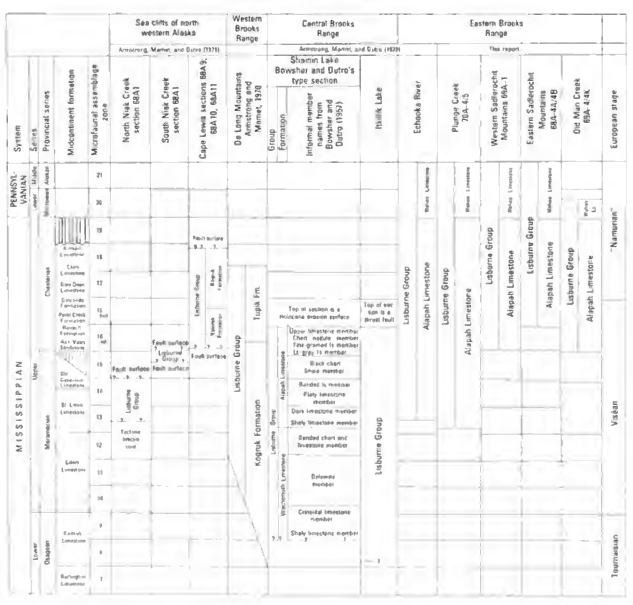

FIGURE 9.—Regional correlation chart for the Lisburne Group of arctic Alaska.

thickness of the Kayak(?) Shale is difficult to determine because of complex faulting at the base of the section.

In the Sadlerochit Mountains and adjacent areas, the Mississippian rock unconformably overlies rocks of Devonian or older age. At the western Sadlerochit Mountains section, the 50 feet of Kayak(?) Shale at the base of the Carboniferous section unconformably overlies the Devonian or older Katakturuk Dolomite (Dutro, 1970). In the other three sections, Carboniferous strata overlie the Neruokpuk Formation, which is Precambrian, Cambrian, and pre-Mississippian (Dutro and others, 1972).

Mamet identified a transition Zone 12/13 Meramecian microfauna at the base of the Alapah Limestone, Plunge Creek section (70A–4/5) (Mamet and Armstrong, 1972). The base of the Alapah Limestone in the western Sadlerochit Mountains 69A–1 section is lower Chesterian, Zone 16$_i$, and in the eastern Sadlerochit Mountains section it is Zone 16$_m$, lower Chesterian. Southeast of the Sadlerochit Mountains at the Old Man Creek section (69A–4/4K), the base of the Alapah Limestone is Zone 16$_i$. The Wahoo Limestone, here of Pennsylvanian age, contains the youngest beds of the Lisburne Group in the report area. In the Plunge Creek,

western Sadlerochit and eastern Sadlerochit Mountains sections, the top of the Wahoo Limestone is Atokan in age, whereas in the Old Man Creek section it is Morrowan.

In the area of this study, the lower (Permian) part of the Sadlerochit Formation unconformably overlies the Wahoo Limestone. Detterman (1970) reported that the basal Echooka Member of the Sadlerochit Formation contains a brachiopod fauna of lower Kazanian, earliest Late Permian age. The unconformity represents a hiatus including Des Moinesian, Missourian, and Virgilian (Pennsylvanian), and Wolfcampian, Leonardian, and possibly lower Guadalupian (Permian) time. The westward thinning of the Atokan carbonate rocks, in the Sadlerochit Mountains (fig. 2) and to the southeast at Old Man Creek, suggests differential erosion, probably owing to differential uplift previous to Sadlerochit Formation sedimentation. At many localities the highest few feet of Atokan carbonate rocks show evidence of vadose weathering in the form of enlarged vertical joints and vugs that are filled with a clay similar to terra rossa. The basal beds of the Echooka Member are conglomerate or conglomeratic sandstone formed partly by rounded chert and limestone pebbles and cobbles derived from the underlying Wahoo Limestone.

REGIONAL RELATIONS OF CARBONIFEROUS CARBONATE ROCKS IN THE SADLEROCHIT MOUNTAINS

Carbonate rocks of the Lisburne Group in the Sadlerochit Mountains and adjacent areas are part of the Carboniferous regional marine transgression of arctic Alaska. Carboniferous rock outcrop patterns in the Brooks Range are shown in figure 1 and in a regional correlation chart (fig. 9). Also shown are the significant exploration wells that have penetrated to the Devonian or older rocks. Brosgé, Dutro, Mangus, and Reiser (1962) defined the northward transgressive nature of the Lisburne Group carbonate rocks in the central and eastern Brooks Range. These studies were continued by Armstrong, Mamet, and Dutro (1970), Mamet and Armstrong (1972), and Armstrong (1974), who also delineated the Sadlerochit high that appears in part to parallel the present-day Sadlerochit and Shublik Mountains.

Armstrong and Mamet (1970) recognized in the Philip Smith Mountains and, from subsurface data, the existence of a thicker accumulation of carbonate rocks in a northeastern-southwestern trend. This negative area of thicker carbonate rocks was named the Canning sag.

The northward marine Carboniferous transgression is shown in carbonate lithofacies maps (fig. 10 and 11) and diagrammatic reconstructed cross sections (fig. 12).

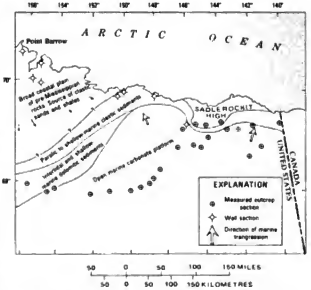

FIGURE 10.—Lithofacies map of northeastern Alaska at the end of Meramecian time.

The residual positive area, the Sadlerochit high, was formed by Devonian carbonate rocks and the metamorphosed clastic rocks of the Neruokpuk Formation. The Sadlerochit high was probably a major source area for clastic material in the Kayak(?) Shale of the region. It remained above sea level through Meramecian time and was finally submerged in early Chesterian time (Zone 16$_8$). The Chesterian carbonate sedi-

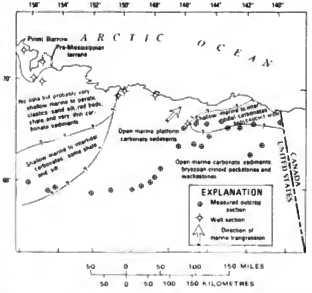

FIGURE 11.—Lithofacies map of northeastern Alaska near the end of Chesterian time.

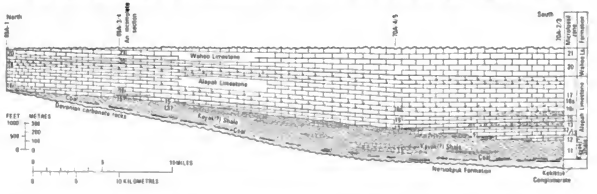

FIGURE 12.—Idealized cross section of the Carboniferous sediments before deposition of the Sadlerochit Formation. The cross section extends southward from section 69A–1, western Sadlerochit Mountains, to the junction of the Canning River and Marsh Fork, sections, 70A–2/3. See figure 2 for location.

ments that overlapped the old Sadlerochit high were deposited in shallow water. Armstrong (1973) reported that intertidal sedimentary structures such as algal mats, birdseye structures, and small lithoclasts are common in the upper part of the Alapah Limestone in the Sadlerochit Mountains (fig. 2).

The diagrammatic cross section (fig. 12) illustrates the northward transgression in the Philip Smith–Franklin Mountains and the onlap over the Sadlerochit high.

The lithofacies maps shown in figures 10 and 11 incorporate subsurface data from exploration wells on the North Slope. Atlantic Richfield/Humble Prudhoe Bay State Well No. 1, near the axis of the Canning sag, has more than 1,250 feet of shallow-water, open-platform carbonate rocks that range from Chesterian (Zone 16) to Atokan (Zone 21) age. The carbonate rocks are underlain by about 550 feet of black and red shale, siltstone, sandstone, and thin coal seams that are probably the Kayak(?) Shale. West of this well (fig. 1) the carbonate sections thin. The Union Oil Kookpuk No. 1 well has about 900 feet of Chesterian to Atokan age carbonate rocks, whereas to the north the Sinclair/British Petroleum Colville No. 1 has only 300–400 feet of Morrowan and Atokan age carbonate rocks. Chesterian age sediments may be represented by about 400 feet of dark-gray to red siltstones, shales, and sandstones, which overlie the pre-Carboniferous argillites. Further west and south of Point Barrow (fig. 1) the United States Navy's wells—Barrow No. 3, Topagoruk, and East Topagoruk—are devoid of Carboniferous carbonate rocks, and above the pre-Carboniferous argillites is a thin sequence of clastic shales and sandstone. These are unfossiliferous but may be of Carboniferous age. No deep tests have penetrated the Carboniferous section south of the Topagoruk well or west of the Colville River. Thus, except for scant aeromagnetic and seismic data, little is known of the subsurface carbonate strata in Naval Petroleum Reserve No. 4 or the area to the west. Projection of Carboniferous outcrops from the De Long Mountains and Lisburne Hills into the subsurface (not shown in figs. 10 and 11) is complicated because in both areas the Carboniferous rock exposures are part of large-scale gravity-slide thrust sheets with dislocations of 60–70 miles in the De Long Mountains (Martin, 1970).

GRAPHIC REGISTRY OF STRATIGRAPHIC SECTIONS

The locations of the stratigraphic sections described in this report are shown in figures 13–16. Maps by Reiser, Dutro, Brosgé, Armstrong, and Detterman (1970) and by Reiser, Brosgé, Dutro, and Detterman (1971) give detailed geologic settings for the sections.

DIAGENESIS

For the purpose of this paper, diagenesis includes all changes that sediments undergo from time of deposition until the present. One of these changes is lithification—that is, the change from unconsolidated sediment to consolidated sediment by compaction, cementation, and pressure solution. As discussed by Purdy (1968) in his admirable summary of environmental factors, diagenesis has necessarily vague limits, and in this study even the localized products of metamorphism along a thrust plane have been included within its realm.

The importance of comparing unconsolidated sediments with their recent lithified counterparts is that processes active at the present time can be extrapolated into the geological past. Although this is the standard procedure of geologic deduction, it must be remembered that variation in sea level in the Holocene, an important

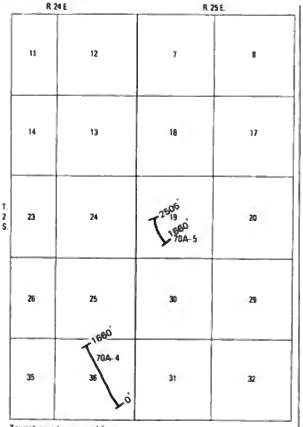

FIGURE 13.—Location map of Plunge Creek sections 70A–4 and 70A–5, Mount Michelson A–4 and A–5 quadrangles.

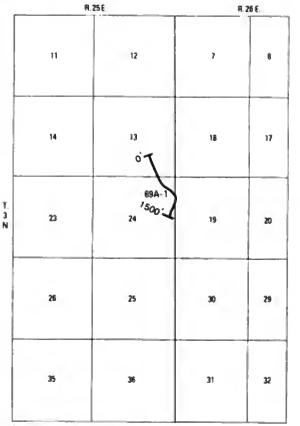

FIGURE 14.—Location map of western Sadlerochit Mountains section 69A–1, Mount Michelson C–4 quadrangle.

parameter in controlling changes in limestone fabrics, is related to the melting of the Pleistocene glaciers. So, at least as far as carbonate diagenesis is concerned, the present is *not* "the key to the past" but rather that "the present is the key to the Triassic[a]"!

CALCITE

The study of calcite fabrics has proved a fruitful method of deciphering the geologic history of limestones. No longer are limestones just limestones to most geologists. Nearly all now appreciate the advantages of subdividing the various limestone rock types on an objective basis as has so universally been accepted for the igneous rocks. In contrast to the subdivision of other major rock groups, nonrecent limestones are now nearly monomineralic, being composed of low-Mg calcite. Recent limestones are composed of two distinct polymorphs of $CaCO_3$ namely calcite and aragonite; the calcite occurs in both low-Mg and high-Mg forms, which contain 0–5 percent and 11–19 percent Mg in solid solution, respectively (Chave, 1954). Both aragonite and high-Mg calcite, the dominant modern carbonate minerals, are metastable under normal conditions, and it is the processes of conversion to stable low-Mg calcite, together with organic influences, that are largely responsible for diversity of fabric types in ancient limestones.

The description of limestones best follows the major subdivision into grains, matrix (carbonate mud), and cement (sparry calcite) used for sandstones by Krynine (1948). This primary subdivision then allows the use of either of the currently most popular and largely objective limestone classification, that is, Dunham (1962) or Folk (1959). The Dunham classification is used throughout this report (as outlined in table 1) because of the genetic significance of mud-supported as opposed to grain-supported limestones.

[a]With affectionate acknowledgment to the late Dr. P. D. Krynine for this analogy between the Permo-Carboniferous and Pleistocene glaciations.

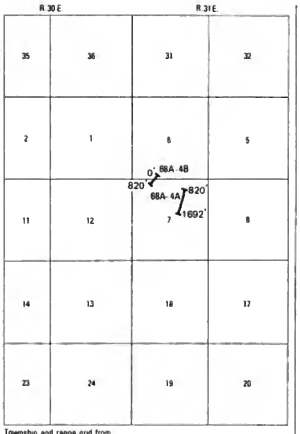

FIGURE 15.—Location map of eastern Sadlerochit Mountains sections, 68A-4A and 68A-4B, Mount Michelson C-1 quadrangle.

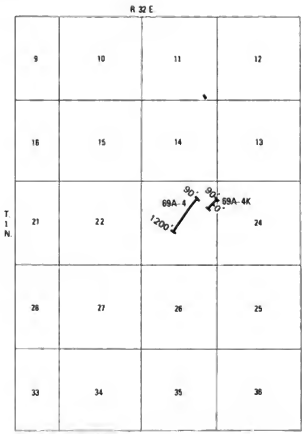

FIGURE 16.—Location map of Old Man Creek sections, 69A-4 and 69A-4K, Mount Michelson B-1 quadrangle.

GRAINS

The grains in the Lisburne Group are largely of bioclastic origin (that is, crinoids and bryozoa) together with the so-called "inorganic" grains such as pellets and oolites.

CRINOIDS

Crinoids are the dominant bioclastic element in the Lisburne Group, and although common throughout the section, they are preferentially developed in the grainstone intervals. The crinoid debris was originally composed of high-Mg calcite, although Schroeder, Dwornik, and Papike (1969) have shown variations between 3 and 43 mole percent of Mg^{2+} in the skeleton. Individual grains are recognized by the rectangular pattern of pores of the spines or by concentric arrangement of dusty inclusions in the columnals surrounded by clear sparry calcite. Although these individual grains optically act as a single crystal, Nissen (1963) suggested that in reality the grains consist of an agglomeration of individual crystals whose *c*-axes are perfectly alined. These "grains" have a spongelike structure with collagen fibers in the hollow spaces (Nissen, 1969). The fact that the skeletal elements of recent crinoids in high-Mg calcite, as well as ancient crinoid debris now preserved in low-Mg calcite, optically act as single crystals implies that the mineralogical conversion takes place on a molecule for molecule basis without large-scale solution. Bathurst (1971, p. 357) pointed out that low-Mg calcite is deposited in the pore spaces of the echinoderms at the same time as first-phase sparry calcite cement. This cementation occurs prior to the loss of Mg^{2+} from the original high-Mg calcite. H. D. Winland (oral commun., 1970) considered it quite probable that the low-Mg calcite syntaxial overgrowth is formed while the echinoderm nucleus is still high-Mg calcite. If, as seems probable, early cementation obliterates the intragranular spaces, it follows that nucleation of intragranular chert (see section on "Intragranular Chert") must have taken place prior to the first phase of cementation.

Evamy and Shearman (1965) described the stages of syntaxial development of sparry calcite by tracing the variation of ferrous iron content. They showed that overgrowths developed preferentially in the direction of the *c*-axes of echinoderm fragments. In the Lisburne Group, however, no iron was found in the overgrowths. The syntaxial cement usually lacks foreign matter (pl. 9, fig. 2); the cement probably formed progressively in space made by pushing aside any intergranular mud.

BRYOZOA

Together with crinoid debris, bryozoan detritus is the most common bioclastic element in the Lisburne Group. In contrast to the observations of Davies (1970, p. 134) in Shark Bay, Western Australia, where bryozoans, although a common member of the biota, are rare as fragments in the sand-size sediments, sand-size detritus of bryozoan fronds are abundant in the Lisburne Group. Although recent bryozoans have either high-Mg calcite or aragonite in their skeletons (Chave, 1954; Sandberg, 1971), in contrast to organisms like pelecypods, the skeletons appear to retain a large proportion of fabric detail through geologic time (pl. 2, figs. 1–5). The zooecia, the living spaces of the organisms, in the Lisburne Group are filled with either carbonate mud or sparry calcite that is independent of the nature of the intergranular material. Reworking is probably indicated where the zooecia are filled with calcite that is different from the intergranular material. In some Lisburne Group samples (pl. 2, fig. 4), the nature of the intrazooecial calcite probably reflects the habit of the original organic material.

OTHER BIOCLASTIC DEBRIS

Other bioclastic debris is rare in the Lisburne Group and consists mainly of pelecypod fragments (pl. 1, fig. 6) and rare solitary corals. These fragments almost invariably do not exhibit the details of the original shell—only the original outline is preserved in a dark thin outer zone that encloses an infilling of sparry calcite cement. This change of texture is related to the solution of the original aragonitic shell and to the subsequent reprecipitation of $CaCO_3$ as low-Mg calcite. The dark outer rim is generally considered (Bathurst, 1971, p. 333) to be a result of the infilling of algal borings by carbonate mud ("micrite envelope"). The preservation of the cast of the original shell after solution and prior to complete infilling by sparry calcite, reveals the possible sequence of alteration of aragonite bioclast debris (fig. 17). As recorded by Logan, Read, and Davies (1970, p. 62) in the Pleistocene Carbla Oolite of Shark Bay, Western Australia, "aragonitic fossils have been dissolved preferentially leaving moldic porosity, whereas calcitic skeletal material remains intact. The molds and intact fossils are set in a matrix of calcitic skeletal debris which is cemented by sparry calcite." Collapsed micrite envelopes have been recorded (Bathurst, 1964), but quantitatively they are rare and have not been observed in the Lisburne Group.

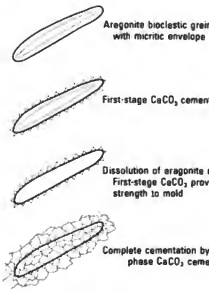

FIGURE 17.—Probable sequence of alteration of aragonite bioclast debris.

Land (1967), as discussed in a later section, showed that the deposition of early-phase sparry cement occurs, mostly as a fringe around the clastic grains, prior to the solution of the aragonite. It is then possible (see pl. 1, fig. 6) that the early cement fringe, together with the micrite envelope, makes the void that results after solution of the aragonite sufficiently rigid to be preserved until it is subsequently infilled by the precipitation of sparry calcite. Winland (1968) has shown that micrite envelopes are sometimes originally composed of high-Mg calcite, whereas Bathurst (1964) stated that an original aragonitic composition is more common. Only rarely is the internal structure of originally aragonitic bioclasts preserved in low-Mg calcite. In these bioclasts the change of $CaCO_3$ polymorph has almost certainly taken place in solution and by immediate redeposition molecule by molecule.

The original internal structure of fibrous pelecypods is, however, sometimes preserved in intragranular chert (see pl. 9, fig. 5), providing further evidence of the early nucleation of this type of chert. The original chamberlets of the probable pelecypod are still outlined by dark inclusions; the presence of these inclusions suggest that they are a remnant after solution of the original shell.

Foraminifera (for convenience included as "bioclastic") occur more commonly toward the base of the

stratigraphic section, especially where the rocks are shaly. They also occur more rarely in the oolite grainstones of the Wahoo Limestone, and their margins appear to grade into intergranular sparry calcite cement.

OOLITES

Oolite grainstones are the dominant rock type in the Wahoo Limestone of all four sections considered in this study. The individual oolites show great variation in shape, and only very rarely do they approach the spherical shape of the ideal oolite. The oolites have a well-developed core, usually a bioclast, while the oolitic skin ranges in thickness from one to four distinct layers. The fabric of the individual oolite skins is both radial and tangential to the core, and only rare patches of the skin are cryptocrystalline calcite. The shape of an oolite is a function of the shape of the bioclastic core: elongate around a pelecypod fragment but equidimensional around a crinoid plate. The thickness of oolitic skins is apparently independent of the shape of the core; in some samples (pl. 1, fig. 2) the thickest oolitic skin occurs around elongate bioclasts, while in others equidimensional grains possess the thickest oolitic coating (pl. 1, fig. 3). The agglutinated foraminifer on plate 1, figure 3, is the only grain in the field of view with no oolitic skin—probably because oolitic growth is difficult on a mineralogically heterogeneous base. In the same field, the core of an oolite is occupied by a single coarse rhomb of dolomite that probably developed after the oolitic coating. Some of the pelecypod bioclasts are now represented by void-filling calcite showing no original fabric. These bioclasts indicate solution of an originally aragonitic shell, leaving a void that was subsequently infilled with sparry calcite cement after the formation of the oolite; the oolite itself was changed to calcite on a piecemeal basis. Compound nuclei, probably originally in the form of detrital carbonate rock fragments, also occur (pl. 1, fig. 2). The encrusting algae *Osagia* is commonly associated with the oolitic facies (pl. 10, figs. 3–5), emphasizing the influence of encrusting organisms in highly agitated environments. Tillman (1971) suggested that *Osagia* is not necessarily associated with shallow water.

Origin of the oolite fabric.—Modern oolites, as those currently being deposited on the Bahama Banks (Newell and others, 1960) and the Trucial Coast of Arabia (Kendall and Skipwith, 1969), are composed of aragonite. Ancient oolites have changed to calcite, the more stable form of $CaCO_3$. This is true of the oolites in the Lisburne Group, but despite this change, the original tangential arrangement of individual crystals has survived. Shearman, Twyman, and Zand Karimi (1970) have clearly shown that retention of the original tangential fabric in oolites is related to tangential crystals of aragonite in a diffuse matrix of organic mucilage separated by distinct concentric layers of mucilage. The transformation of aragonite to low-Mg calcite apparently takes place in solution molecularly, and this process allows the fine detail of the concentric layers of mucilage to be preserved. The calcite tends to develop perpendicular to the surfaces of the concentric mucilage layers to form radial partitions with their c-axes parallel to their length, pushing aside the diffuse mucilage (see fig. 18). It therefore is obvious that the radial fabric so common in oolites is a diagenetic rather than a primary feature. The rare patches of cryptocrystalline calcite are probably produced by local large-scale solution of aragonite; this process would leave the mucilage layers unsupported and permit their collapse, or as suggested by Twyman (1970), the calcite may infill the cavities created by algal boring.

Cementation of oolites.—As mentioned in the previous section on depositional environments, oolites are formed by high-water energy on shoals or deltaic flats from which available carbonate mud has been winnowed. This process implies that most oolitic rocks are of the grainstone type with most of the intergranular space available for subsequent sparry calcite cementation. The rarer specimens of oolites that are associated with carbonate mud have probably been moved from the site of their formation. Their cementation history differs little from other clastic grains, but examples of oolitic skins detached from their core (pl. 1, fig. 4) provide good evidence that compaction occurred before the

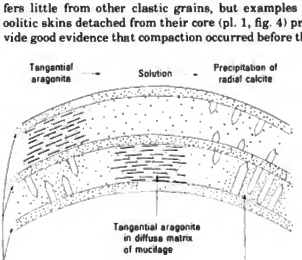

FIGURE 18.—Diagram showing the alteration from tangentially arranged aragonite crystals to radially arranged calcite crystals within the concentric mucilaginous layers of an oolite (from Shearman and others, 1970, fig. 4).

major second phase of cementation. The original core is outlined by first-phase sparry calcite crystals with *c*-axes at right angles to the inner surface of the oolite skin. Displacement of the oolite skin from the core took place along two planes of movement, probably the result of compaction. The newly formed void adjacent to the original core and the remainder of the core itself were later filled with equant second-phase sparry calcite cement. As with similar examples described by Shearman, Khouri, and Taha (1961) from the Jurassic limestones of the French Jura, early-phase cement is poor in iron and is related to the aragonite-low-Mg calcite transition, but the second-phase cement is rich in iron.

Mechanism of oolite formation.—The mechanism of oolite formation is still a matter of dispute, but the presence of an organic matrix in oolites similar to that, for example, in pelecypod shells suggests that it is not a purely inorganic process.

The classical hypothesis for the development of oolites is the snowball mechanism, described by Sorby as early as 1879, which involves the accretion of aragonite needles on a nucleus in shallow sea water supersaturated with $CaCO_3$, which, as a result of constant rolling, would allow the development of concentric layers. This theory discounts any influence of the organic matrix in oolitic development, and in addition, Donahue (1965) has pointed out that the highly polished outer surface of growing oolites is difficult to reconcile with a hypothesis of mechanical accretion. Twyman (1970) stated that "the high degree of surface lustre of oolites is not necessarily due to abrasion. It seems rather more likely that the thin skin of organic matter which characteristically coats nearly all oolite grains in the Al Bahrani delta of Abu Dhabi acts like a coat of varnish to make the oolite grains shiny."

The similarity between the nature of the organic content of calcium carbonate skeletons of invertebrates and oolites is the clue to the biochemical origin of the original oolitic aragonite. Simkiss (1964) and Kitano and Hood (1965) have shown that the nature of the organic matrix is the main influence on the calcium carbonate polymorph formed during construction of the shell. This matrix is composed of a peptide-polysaccharide complex that "provides nucleating sites for $CaCO_3$ either by acting as a template for epitaxial nucleation or by its ability to attract the appropriate inorganic ions electrostatically" (Mitterer, 1971, after Wilbur and Simkiss, 1968). Although epitaxis is probably the dominant mechanism of test or skeleton construction in $CaCO_3$, Blow and Brooks (1975) consider that a nonepitaxial mechanism, whereby the formation of largely organic colloid systems may act to concentrate $CaCO_3$ on micelle structures (Duck, 1966), may be more appropriate for some Foraminifera. Mitterer (1971) illustrated a series of amino acid chromatograms of the chlorophyte alga *Halimeda*, three mollusks, and two specimens of modern oolites (all of which are originally aragonitic). Not only is the amount of protein in the oolites of the same order of magnitude as that of the mollusks (2–4 micromoles per gram of $CaCO_3$), but there is also a remarkable similarity in the overall chromatograph pattern. Aspartic acid, glycine, alanine, leucine, and lycine are the dominant amino acids in the algae, mollusks, and oolites. Unfortunately, Mitterer (1971) does not refer to the sampling location of the algae and mollusks, and therefore the possibility that the distribution of amino acids is related to the environment rather than to the species independent of environment cannot be completely discounted. The above argument, especially in view of the evidence that calcium carbonate does not precipitate inorganically on coated grains (Chave and Suess, 1967) suggests that the origin of oolites has a large biochemical element. Mitterer (1971), however, has pointed out that if the argument is taken further, oolites would be expected wherever organically coated grains occur in water supersaturated with $CaCO_3$. This does not agree with the facts. Further work on the distribution of organic matter in carbonate shoal areas is necessary before this question can be completely resolved.

PELLETS

The pellets in the Lisburne Group are well distributed throughout the Alapah Limestone but are rare in the Wahoo Limestone. In general, pellets are concentrated in wackestone and packstone rock types and occur only sporadically in grainstones. The pellets are homogeneous in internal fabric, and their well-rounded outlines tend to be preserved. There is no evidence to suggest that the pellets are anything but fecal remains. But no trace remains of the organisms that produced the pellets.

CEMENT

Cement is defined as an intergranular material introduced into the rock as a precipitate from interstratal solution, and it is not the product of clastic sedimentation. To provide for the introduction of cement, it is necessary to have a framework that will preserve void spaces prior to cementation. The most common framework in carbonate rocks is a grain-contact fabric, that is, grainstone of Dunham (1962), where intergranular carbonate mud is almost absent. Another framework that permits the introduction of cement is an already lithified carbonate rock from which the more soluble mineral has been taken into solution, for example, voids after aragonite shells in a calcite host or voids after calcite clasts in a dolomite host.

SPARRY CALCITE CEMENT

Primary pore space, that is, intergranular space, is absent from the Lisburne Group. In grain-contact rocks, where there is little or no carbonate mud, the potential pore space has, without exception, been obliterated by sparry calcite cement. In mud-supported rocks, sparry calcite cement exists only as a void filling after solution of originally aragonitic shells. Winnowing in a high-energy environment allows the available carbonate mud to be removed to a lower energy environment.

The distribution of sparry calcite cement in the grainstones of the Lisburne Group is discussed in the section "Environments of Deposition." The depositional environment of the cemented grainstones is considered to have been a shallow-water shoal. Grainstones, except for a 400-foot interval toward the base of the western Sadlerochit Mountains section (69A–1), are rare in the Alapah Limestone. In the Wahoo Limestone, however, completely cemented grainstones (often oolitic) are the dominant rock type. Two distinct phases of sparry calcite cement are apparent in the Lisburne Group. The first-phase cement forms a thin fringe of relatively constant thickness (~30μm) around the clastic carbonate grains (see pl. 1, figs. 1–6) with stubby crystals with pyramidal terminations growing at right angles to the grain margins or as syntaxial overgrowths on echinoderms. In recent limestones these early fringes are part of Stage II of Land's six stages of cementation (Land and others, 1967), usually formed by meteoric water above the water table (that is, vadose zone). The nature of the fringe cement in recent grainstones appears to be a function of access to salt water. In the intertidal zone the beach rock cement is either aragonite or high-Mg calcite, whereas away from the marine influence, the meteoric environment produces a low-Mg calcite fringe cement (Bathurst, 1971, p. 368).

Although the fabrics recorded from recent limestones are comparable with those of the Lisburne Group [cf. the isopachous beach rock cement of the Pleistocene Belmont Formation of Jamaica (Land, 1971, p. 135)], it is not possible to assess the original mineralogy of the early-phase cement in the Lisburne Group. A fossil example comparable to that found in the Lisburne Group is the "short, closely packed, calcite druse" described by Purser (1969) from the Middle Jurassic of the Paris Basin, and it is suggested as being originally calcitic.

Except for the two zones of dedolomitization (see section on "Environments of Deposition"), or the intertidal algal mat of the eastern Sadlerochit Mountains section (68A–4A/4B), there is no evidence of breaks of sedimentation in the Lisburne Group. Thus, in general, although the Lisburne early cement has textural analogies with recent examples from a vadose zone, it probably formed in a subtidal environment. This cement probably originated as a precipitate of calcium carbonate from supersaturated tropical sea water, as described by Taylor and Illing (1969) and Shinn (1969) in the Arabian Gulf.

Second-phase sparry calcite completely obliterates the available pore space with subequant crystals that are much coarser than the first-phase cement. Crystal size tends to increase toward the center of a void fill. There appears to have been a time lapse between the two phases of cement, the second phase of which tends to be rich in Fe^{2+} (as discussed in the section "Fe^{2+} in Calcite"). The evidence from oolitic skins displaced from the now dissolved core (pl. 1, fig. 4) and the existence of enfacial junctions (Oldershaw and Scoffin, 1967; Bathurst, 1971, p. 434) support this view. The second-phase cement presumably formed after the conversion of all metastable carbonate minerals to low-Mg calcite (part of Land's stage IV of cementation (1967)).

Internal silts similar to those described by Dunham (1969) from the Permian limestones of New Mexico and ascribed to the vadose zone are absent from the Lisburne Group. This fact, together with the apparent continuity of sedimentation, suggests that the second-phase cement developed in a phreatic environment.

The source of the $CaCO_3$ necessary for complete cementation implies that the second-phase cement, at least, is from a distant source (analogous to the distant-source dolomite of Murray, 1964). Bathurst (1971, p. 457) suggested that neither solution of local aragonite, especially in view of the lack of collapsed micrite envelopes, nor pressure solution will provide sufficient volume to obliterate the intergranular space. But if submarine precipitation of $CaCO_3$ is invoked, then the regional distribution of sparry calcite is left unexplained.

Illing, Wood, and Fuller (1967) suggested that the relative amount of available second-stage sparry calcite cement is partly a function of the tectonic setting of the area. For example, primary intergranular porosity is very common in the limestones of the Arabian Gulf where continuous calcareous sedimentation has persisted throughout most of the Mesozoic and Tertiary eras, whereas in North America, where interrupted cratonic limestone deposition is dominant, very little primary pore space has escaped cementation by sparry calcite.

At the conclusion of this discussion, however, we still have no answer as to the origin of the second-phase cement. We can only suggest that a very large proportion of originally aragonitic bioclasts, without micrite envelopes, has gone into solution and has disappeared from the geological record. This process could provide a very large amount of cement and would also explain its regional variation in distribution.

NEOMORPHIC PROCESSES

Neomorphism (Folk, 1965) is an increase or decrease in crystal size. For calcium carbonate, this generally involves a change of lattice type (for example, the change from aragonite to low-Mg calcite) and it has been dealt with in the preceding discussion. It also includes a change in crystal size without change of lattice type, a process usually referred to as recrystallization. The product of the latter process is either aggrading or degrading in form and, in our experience, is quantitatively of minor importance.

The operational criteria for recognizing neomorphic spar have been outlined by Bathurst (1971, p. 484); he also emphasized that recrystallization is a wet rather than a dry process. Aggrading neomorphic fabrics have not been positively recognized in the limestones of the Lisburne Group, but this process is invoked to explain the grain size of probable syngenetic macrodolomites. The average grain size of recent syngenetic dolomites is about 4μm (L. V. Illing, oral commun., 1970), whereas macrodolomite grains of the Lisburne often exceed 50 micrometres, and even the microdolomite grains commonly are larger than 10 micrometres. These sizes suggest that an aggrading process operates in dolomite through geologic time, the maximum grain size achieved being a function of the available pore fluids.

The only positive evidence of degrading neomorphism is illustrated on plate 6, figure 1; the illustration shows that the crystal size in a crinoid plate and its syntaxial overgrowth has decreased while the matrix (probably originally carbonate mud) and bryozoan fragments have increased in grain size. In the end stage of neomorphism, this rock would be a dusty equigranular calcite mosaic from which all evidence of bioclastic remains has been eliminated. The formation of marble (see the section on "Marble") after thrust movement is a process closely analogous to sedimentary neomorphism except that large-scale stress is the trigger mechanism for annealing the crystals.

MATRIX

Matrix is defined as intergranular material. It is usually composed of carbonate mud (micrite) and is dominantly of clastic origin. The separation of grains and matrix is to some extent a function of the scale of observation, but in practice a tendency toward a bimodal size distribution in micritic limestones makes the distinction easy. Individual crystals of micrite have an upper size limit of 3–4 micrometres (Bathurst, 1959).

Carbonate mud is the dominant intergranular material in the Alapah Limestone, although toward the base of the Plunge Creek section (70A–4/5) the matrix contains a relatively high proportion of clay minerals.

Recent carbonate mud is largely bioclastic in origin, whether originally mainly aragonitic (as described in Cloud, 1962, from the Bahamas) or calcitic in composition (Davies, 1970, Shark Bay, Western Australia). The only known inorganic precipitation of $CaCO_3$ is in the lagoons of Abu Dhabi (Kinsman and Holland, 1969).

Ancient micrites usually have a porosity of about 1 percent, although chalks have porosities as great as 40 percent. The process by which recent carbonate mud with porosities in excess of 50 percent becomes lithified is a matter of some complexity.

Although Wolfe (1968) demonstrated a 30-percent reduction in volume during the diagenesis of the Chalk of Northern Ireland, evidence of compaction is generally lacking in limestones. This would then imply that to complete the process of lithification, the $CaCO_3$ has an external source. It is, however, difficult to visualize this process because the low porosity micrites (~ 1 percent porosity) have a permeability of about 0.01 millidarcies, and even the high-porosity chalks have low permeabilities (less than 10 mD). These figures suggest that very small amounts of carbonate-rich interstratal solutions pass through the carbonate mud. The most probable origin of excess $CaCO_3$ is, in our opinion, within the carbonate mud itself—a process of solution and almost immediate redeposition that allows reduction of the original volume without obvious signs of compaction. This process probably is most active in rocks with an original high aragonite content. In contrast, rocks composed originally of low-Mg calcite (for example, chalk is composed essentially of skeletons of coccolith debris) have little tendency to this small-scale solution, and in general the porosity tends to be retained during geological time.

DOLOMITE

The double carbonate of calcium and magnesium (dolomite) contrasts with calcium carbonate in having only one crystallographic form (euhedral/anhedral rhombs). As mentioned in the previous section on "Calcite", the conversion of metastable aragonite or high-Mg calcite to stable low-Mg calcite commonly causes ground water to become enriched in calcium carbonate; this calcium carbonate is subsequently deposited as sparry calcite cement. Dolomite, except for the relatively rare process of dedolomitization, is not subject to large-scale solution, and dolomite-rich interstitial waters are rare. These chemical and mineralogical factors together with the absence of dolomite as a primary constituent of marine skeletons explain the paucity of diagenetic information obtainable from dolomite fabrics.

The major source of variability in dolomites is in the degree of nonstoichiometry. Ideally, dolomite has a 1:1

ratio of Ca/Mg, but when ferrous iron is incorporated into the dolomite lattice, it substitutes more readily for Mg^{2+} ions than for the Ca^{2+} ions. Katz (1971) reported that calcian-ferroan dolomites averaging $Ca_{56}Mg_{35}Fe^{2+}{}_7(CO_3)_{100}$ are common in the Mahmal Formation of southern Israel, and in 1968 he suggested that these non-stoichiometric dolomites are particularly prone to dedolomitization. Another nonstoichiometric form, but one that does not incorporate foreign ions into the dolomite lattice, is protodolomite, which contains about 10 mole percent of excess $CaCO_3$ in the lattice (Goldsmith and Graf, 1958). Protodolomite, of composition $Ca_{56}Mg_{44}$, is deposited in the Coorong Lagoon of South Australia (Alderman and Skinner, 1957) and is common in the recent dolomites of the Arabian Gulf sabkhas (Kinsman, 1966). Illing, Wells, and Taylor (1965) record recent dolomite rhombs of the size 1–5 micrometres from Qatar in the Arabian Gulf. In spite of their comment that they were dealing with "true dolomite," their data showing the existence of dolomites with a Ca:Mg ratio up to 55:45 are comparable to the protodolomites of the Coorong Lagoon (Alderman and Skinner, 1957). Wood and Wolfe (1969) have described Jurassic-Cretaceous rocks from Abu Dhabi that were deposited in an environment similar to those from Qatar, but the dolomite rhombs average 50 micrometres in size, suggesting that extensive grain growth has taken place during diagenesis—a process that could be associated with the loss of Ca^{2+} from the original protodolomite. In general, protodolomites probably lose their excess Ca^{2+} and gradually revert to the stoichiometric composition.

DOLOMITE

Dolomite is best subdivided on the basis of its grain size. Following the usage of Illing, Wood, and Fullor (1967), the dolomites are subdivided into *macrodolomite*, which has an average grain size larger than 30μm, and *microdolomite*, which has an average grain size of smaller than 30 μm. As discussed in the section on the "Origin of Dolomites", the distinction between syngenetic and diagenetic dolomites is difficult to determine, but the average grain size is one factor that helps.

As described in the section 69A–4/4K, Old Man Creek, the Plunge Creek section (70A–4/5) has the largest amount of dolomite in the total section (33 percent) as compared with 9 percent in the western Sadlerochit Mountains (69A–1) and 15 percent in the east Sadlerochit Mountains (68A–4A/4B). The dolomite is concentrated in all three sections of the Alapah Limestone, and rare amounts are present in the dominant grainstone rock type of the Wahoo Limestone.

In the Plunge Creek section, the lower of two predominantly dolomite units (330–720 ft) is homogeneous unzoned macrodolomite with rare intervals of microdolomite; the upper unit (918–1,630 ft), which terminates the Alapah Limestone, is dominantly macrodolomite interbedded with wackestone and packstone (fig. 2). The macrodolomite rhombs of the lower unit are often outlined in hematite, and toward the top all interrhombic spaces are filled with dark clay. Iron-rich cores are sporadically apparent in the rhombs. Dolomite is a common accessory in the limestone, and at those places where it occupies less than 25 percent of the total volume, the grain size tends to be coarser.

In the western Sadlerochit Mountains section (69A–1) five thin discrete units of 10–20 feet of dolomite, largely microdolomite, are scattered through the Alapah Limestone. No thick units of dolomite exist in this section although the suggested depositional environment of the uppermost unit of the Alapah Limestone is a restricted platform, similar to that suggested for the uppermost dolomite unit in the Plunge Creek section. Accessory macrodolomite rhombs are common. They are usually outlined with hematite, and some have an iron-rich core with iron-poor rims.

In the eastern Sadlerochit Mountains section (68A–4A/4B), the total section contains 15 percent of dolomite concentrated in two major units of the Alapah Limestone. The lower unit (360–520 ft) consists of homogeneous macrodolomite with an absence of zoning in the individual rhombs. The upper unit (750–820 ft), which terminates the Alapah Limestone, consists of a microdolomite with patches of chert. Algal mats have been recorded in the outcrops of this unit. Scattered discrete horizons of microdolomite with remnants of bryozoan and crinoid debris occur in the Wahoo Limestone. Patches of iron-rich macrodolomite in a microdolomite host (pl. 3, fig. 9) represent a later stage replacement of a high-Mg bioclast such as a crinoid plate.

In the Old Man Creek section (69A–4-4/K), a large proportion of the rocks are dolomite, but as mentioned in the section on "69A–4/4K, Old Man Creek," they have been subjected to intense recrystallization. Microdolomite (some of which is laminated) is the major rock type, and it is particularly well developed at the top of the Alapah Limestone (940–1,032 ft) and toward the base (0–215 ft). The macrodolomites tend to be sporadic thin beds, and many individual rhombs have cloudy cores with clear rims.

ORIGIN OF DOLOMITES

The origin of dolomite, long a matter of dispute, has been largely resolved since the advent of X-ray spectroscopy and detailed fieldwork in areas of recent dolomite formation such as the island of Bonaire in the Netherlands Antilles and the coastal flats (sabkhas) of Abu Dhabi. The source of the excess Mg^{2+} ions needed to

produce dolomite is now accepted as interstitial brines in which the Mg/Ca ratio has been increased.

Whether or not primary dolomite exists is largely a semantic argument regarding the definition of "primary." The earliest formed dolomite is usually referred to as syngenetic, that is, formed prior to lithification as a dolomite mud. The production of the high Mg^{2+} ratio is produced in areas where evaporation exceeds precipitation. These heavy brines then seep down into the underlying sediments, which become progressively dolomitized (Adams and Rhodes, 1960; Deffeyes and others, 1965).

Syngenetic and diagenetic dolomites are certainly the most important types, although detrital and epigenetic dolomites are also described in the literature (Friedman and Sanders, 1967). The distinction between syngenetic and diagenetic dolomites is, however, often difficult to make. It is possible to establish criteria for each type, but they are by no means mutually exclusive.

Syngenetic dolomite

1. Very fine grain size (~10μm), which can be increased by a process of grain growth.
2. Homogeneous nature of the individual crystals and the rock itself.
3. Association with sulfate minerals or with evidence of intertidal environments (algal mats).
4. Restriction to one horizon, commonly at the end of a depositional cycle.

Diagenetic dolomite

1. Medium to coarse grain size.
2. Individual crystals; often zoned and have more than one phase of dolomite formation.
3. Partially dolomitized rocks are common, and the dolomite may be in the lime-mud matrix rather than in the grains themselves.
4. Interdigitation with nondolomitic carbonate rocks.

For the Lisburne Group of the Sadlerochit Mountains, in particular, the most reasonable conclusion is that both syngenetic and diagenetic dolomites exist. The syngenetic type is associated with the top of the dolomite unit that commonly occurs at the top of the Alapah Limestone and below the shallow-water grainstone of the Wahoo Limestone.

A supratidal-intertidal environment has already been postulated for syngenetic dolomites from the occurrence of algal mats. The dolomites that fulfill the criteria for a diagenetic origin tend to occur below those of probable syngenetic origin and could well have been formed by some form of reflux of heavy brines. As discussed in the section on "Chert", the dolomite that occurs in chert is thought to be associated with the development of chert and is independent of normal dolomitization processes. Epigenetic dolomite is probably represented by central dolomite fillings of fractures lined on both sides with quartz (pl. 3, fig. 2) and by the development of dolomite in bitumen restricted to planes of stylolites (pl. 12, figs. 1, 2). Müller and Tietz (1971) illustrated an example of the dolomitization of early-phase sparry calcite rim cement that leaves the equant second-phase sparry calcite unaffected. The bioclastic grainstone section (pl. 4, fig. 4) from the western Sadlerochit Mountains may be another example of this phenomenon.

ZONING IN MACRODOLOMITES

The zoning of dolomite crystals, similar to the zoned macrodolomites of the Lisburne Group, has been discussed in detail by Katz (1971). He suggests that the zoning represents growth stages of the rhombs and that the variation in composition of each zone reflects "compositional changes in the interstitial brines with respect to their dissolved Ca^{2+}, Mg^{2+} and Fe^{2+} contents during dolomite crystal growth."

Although zoning is common in the Lisburne Group macrodolomite, it is difficult to be sure of the original mineralogical nature of each of the zones. Figure 19 illustrates a possible origin of the macrodolomite in the Lisburne Group, although it must be emphasized that iron-rich cores (recognizable from a potassium ferricyanide stain) are by no means ubiquitous. The first stage is the formation of accessory iron-rich dolomite—probably in carbonate mud trapped within the dominantly bioclastic grainstones and prior to any sparry calcite cementation (Stage 1). The ferroan dolomite is nonstoichiometric and contains excess calcium relative to magnesium. This type of dolomite is particularly prone to dedolomitization because of either the increase in free energy of calcian dolomite relative to normal dolomite or the ease of replacing calcium ions through the intercrystalline boundaries (Katz, 1968).

When the calcian-rich zones have been replaced by calcite (Stage 2) or with the approach of ferroan dolomite to a stoichiometric composition, it is probable that the excess of iron in the calcite lattice will then be expelled to the rim of the dolomite rhombs. This expelled Fe^{2+} is in the form of ferric oxide (Stage 3). A second stage of dolomite (Fe free) is sometimes deposited around the original rhomb and in optical continuity with it (Stage 4), that is, the external-source dolomite of Murray (1960). The core of the dolomite rhomb is then susceptible to solution as shown by the existence of iron-stained rhombs with a patchily dedolomitized rim but either a void or a corroded non-Fe dolomite core surrounded by a void "moat." Solution almost certainly occurs after the pore-fill stage of sparry calcite deposi-

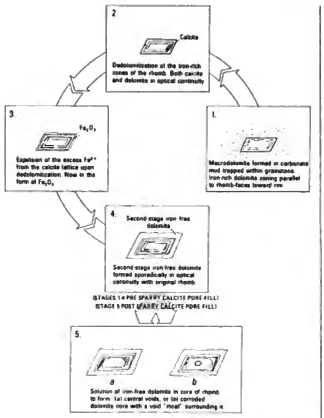

FIGURE 19.—Sequence of diagenesis in zoned iron-rich dolomites.

tion because infilling of voids formed by solution has not been observed.

This interpretation differs from that given by Katz by suggesting that the hematite-rich outer zone is related to the expulsion of Fe^{2+} from original ferroan dolomite zones and not, as suggested by Katz, to direct precipitation directly from interstitial solution upon growing dolomite crystals. The main factors supporting this conclusion are that (1) the hematite zones are developed on the outer margin of the first phase of dolomite formation, and (2) hematite is particularly well developed when zones of dedolomitization are apparent.

DEDOLOMITE

A characteristic of dolomite as an accessory mineral is its occurrence as discrete rhombic crystals. Since the widespread use of the organic Alizarin Red S stain (Friedman, 1959) has facilitated the distinction between calcite and dolomite, several authors have described the replacement of such dolomite rhombs by calcite (Shearman and others, 1961; Schmidt, 1965; Bausch, 1965; Evamy, 1967; Armstrong, 1967; Mattavelli and others, 1969).

Dedolomites are found in the Lisburne Group of the Sadlerochit Mountains. They occur in two major types. The most common type is the selective replacement of dolomite in planes parallel to and toward the outer margin of the original rhomb faces (see pl. 5). The most common example of this type is a discrete dolomite rhomb outlined in hematite with one thin plane of calcite parallel to the rhomb faces. In some rhombs the interiors are dolomite, but in others the cores are voids (see pl. 4, figs. 4, 5, 6).

In the example in the frontispiece and on plates 4 and 5, the diagenetic history is apparently more complicated. The dedolomitized calcite is developed in a series of planes parallel to the rhomb faces and is concentrated toward the outer edge. The calcite is not in optical continuity with the original dolomite, and its extinction is patchy. The variation in the orientation of the calcite is noticeable in the difference in the orientation of the twin planes; these orientations could be secondarily induced. The iron-poor original dolomite rhomb extinguishes in quadrants and is in optical continuity with adjacent overgrowths of dolomite. The terminations of the overgrowths are parallel to the plane intersection of the original rhomb faces. Patches of hematite occur on the edge of the rhomb.

Simple, partly dedolomitized rhombs of this type occur in a zone (550–558 ft) of the Plunge Creek section where not only is a zone of calcite developed toward the outer edge of the rhomb, which is outlined in hematite, but the outer margin is etched by the adjacent sparry calcite cement.

Other examples of this type of dedolomitization were found in the western Sadlerochit Mountains section (69A–1). The coarse-zoned dedolomites of plate 5 occur between 60–80 feet. Between 445–465 feet (pl. 4, fig. 5) the rhombs outlined in hematite have a single zone of calcite toward the outer margin of the rhomb, and in addition the center of the original rhomb is now void.

The second type of dedolomitization is the spotty replacement of dolomite rhombs by calcite. The arrangement of the calcite spots is not apparently related to the structure of the individual rhombs. The outer margins of the rhombs are commonly corroded by adjacent sparry calcite. This second type of dedolomite is restricted to the Old Man Creek section (69A–4/4K) (pl. 4, fig. 7).

CAUSES OF DEDOLOMITIZATION

Von Morlot (1848) suggested that the conversion of dolomite to calcite possibly resulted from the reaction of calcium sulfate-bearing solutions on dolomite, that is,

$$CaCO_3 \cdot MgCO_3 + CaSO_4 = 2CaCO_3 + MgSO_4.$$

Tatarskiy (1949) suggested that this is a valid process but found it restricted to outcrops.

De Groot (1967), however, has shown from experiments that dedolomitization can be achieved by a high Ca^{2+} Mg^{2+} ratio, and Fritz (1967) suggested that dedolomitization is probably taking place in the German Jura at the present day. Katz (1968, 1971) considered that calcian dolomites are particularly susceptible to dedolomitization. In the case of the Mahmal dolomites of Israel, Katz suggested that dedolomitization takes place during intervals of dolomite growth. Even if dedolomitization is accepted as being restricted to surface outcrops, it is not normally known whether the dedolomites are of recent or ancient origin. Schmidt (1965) and Braun and Friedman (1970) have used zones of dedolomite as possible indicators of unconformity surfaces, but none of the examples cited by them prove that the dedolomitization was not modern.

The dedolomite in the Lisburne Group of the western Sadlerochit Mountains section (69A–1) (pl. 5) can only be explained in terms of a dedolomitization process operative prior to formation of secondary dolomite overgrowths. If ancient dedolomitization is accepted as a clue to an unconformity surface, then the dedolomite of 60–80 feet in section 69A–1 is probably an example. Correlation on the basis of Mamet's foraminiferal zones of this zone of dedolomitization in the western Sadlerochit Mountains section (69A–1) ties in with the dedolomitization zone from 550–558 feet in the Plunge Creek section (70A–4/5), that is, within Zone 16; of the Chesterian Series. This correlation is an added indication that both these dedolomitization zones could be a product of meteoric waters with a high Ca^{2+} / Mg^{2+} ratio produced during a period of emergence. There is no evidence that the upper zone of dedolomitization in 69A–1 (that is, 455–465 ft) is other than a product of recent meteoric waters. Indeed the preservation of intra-rhombic voids alone would suggest that solution of the dolomite took place after the formation of the sparry calcite cement.

The spotty dedolomite common in the Old Man Creek section (69A–4/4K) almost certainly has a different origin. As described in the section on "69A–4/4K, Old Man Creek" the limestones of section 69A–4/4K have been subjected to extensive metamorphism attributed to the emplacement of the Mount Michelson pluton. This metamorphism has resulted in widespread grain interpenetration and solution of calcite. The dedolomitization would then probably be a result of the resulting interstitial fluids with a high Ca^{2+} /Mg^{2+} ratio.

DISTRIBUTION OF IRON

Although the presence of trace cations (especially ferrous iron) in both dolomite and calcite is well known, it is not normally detectable in thin section. Iron more commonly enters the dolomite lattice, and the end member is the iron-calcium carbonate, ankerite, where all the magnesium ions have been replaced by ferrous iron with a consequent increase in both refractive index and birefringence.

Evamy (1963, 1969) and Evamy and Shearman (1965, 1969) not only described a reliable and stable stain for locating iron in the carbonate lattices but also used this distribution to draw petrogenetic conclusions. The preferred stain for ferrous iron is 0.5 percent saturated potassium ferricyanide in a 0.2 percent solution of hydrochloric acid, which provides a blue ("Turnbull's blue") pigment. The intensity of the stain is in direct proportion to the concentration of ferrous iron, other factors being equal. This potassium ferricyanide stain was used regularly in the study of the Lisburne Group. More recently, Freeman (1971) has used cathodoluminescence to distinguish between different phases of cement that possess more subtle variations of Fe^{2+} content than is traceable by the potassium ferricyanide stain.

Fe^{2+} IN CALCITE

The distribution of iron in the calcite of the Lisburne Group appears to follow a uniform sequence. The debris (bioclastic, oolitic, and pelletoid) appears to be essentially free of iron, and this is also true of any interstitial mud (micrite). Two generations of sparry calcite can, however, sometimes be clearly separated on the basis of their iron content. The first phase of sparry calcite forms either as iron-poor syntaxial overgrowths around echinoderm fragments or as fringes around other bioclasts or oolites. Evamy and Shearman (1969) clearly demonstrated that the overgrowths on echinoderm crystals are developed as iron-poor spires of crystals in the direction of the *c* axis of the original grain. The serration of the outline of the first-phase sparry calcite is a result of the initiation of cementation only on the fragment surface between the pore-canal openings. Overgrowths tend to be restricted to those parts of the original crystal that allow growth parallel to the *c* axes. Grain relations shown on plate 9, figure 2, suggest that syntaxial overgrowths on echinoderm debris are a result of the pushing aside of original detritus rather than being a product of replacement. The first-stage iron-poor sparry calcite overgrowths on pelecypod fragments and oolites also tend to be of irregular prismatic outline elongated at right angles to the grain surface. In contrast, the first-stage cement is not noticeable around bryozoan fragments. The introduction of second-stage sparry calcite represents the final phase of obliteration of the original pore space of the grainstones. The calcite occurs as generally equant crystals, the orientation of which ignores the shape of the pores. Although variable, this second-phase cement tends to be rich in iron, but in any one thin section no zoning of the iron content

was apparent; this lack of zoning contrasts with that described by Evamy and Shearman (1969). The concentration of iron in the second-phase sparry calcite cement is at a maximum in the coarse grainstone units of the Lisburne Group, especially in the oolite units of the Wahoo Limestone. Although it has been observed that the lime mud (micrite) generally shows no evidence of the presence of Fe^{2+} at 990 feet in the eastern Sadlerochit Mountains section (68A–4A), the micrite adjacent to some patches of chert is particularly enriched in ferrous iron (pl. 8, fig. 4). This suggests that the zone of Fe^{2+} enrichment could represent concentrations of all the iron originally in the replaced limestone.

The time relationship between the two stages of calcite cementation is of importance. There is no evidence of corrosion prior to stage two or any suggestion of a plane of inclusions that could define the termination of stage one. Nevertheless, the change of habit coincident with the general increase in iron content in the second stage suggests some time lag between the two stages of cementation. Enfacial junctions (Bathurst, 1971, p. 434) are common between the iron-rich and iron-poor phases of cementation in the Lisburne Group and could provide support for a time difference between the stages of cementation. An example of the early fringe, iron-free, first-phase calcite cement growing perpendicular to the oolite surface with the absence of second-stage cement is illustrated in Illing, Wood, and Fuller (1967, fig. 1F) from the oil-bearing Minagish Oolite of Kuwait.

Fe^{2+} IN DOLOMITE

As described in detail in the previous section, the dolomite in the Lisburne Group is of at least two distinct generations. The early first stage is often iron rich, in contrast to the sparry calcite. Some of the samples of this phase are homogeneously rich in iron and remain rich in iron with time (60 ft, 69A–1); they occur as the iron-rich and "dusty" core to dolomite rhombs (pl. 4, fig. 8) or as corroded homogeneous iron-rich dolomite (pl. 4, fig. 2). More common, however, is the presence of clusters of iron-oxide-rimmed rhombs that appear to be zoned and probably represent original-zoned ferroan dolomite that has readjusted to its lattice to expel the contained iron. This zoning is particularly noticeable with zones of dedolomitization parallel to the rhomb faces (+60 ft, 69A–1).

The second-stage dolomite occurs either as an iron-free rim around the ferroan dolomite core or as iron-free overgrowths developed along the plane of intersection of the rhomb faces. This second stage postdates any phase of dedolomitization (pl. 5). A possible third phase of iron-free dolomite occurs in section 69A–1 where veinlets crosscutting the host rock are partly filled with dolomite.

TABLE 3.—*Habit and iron content of sparry calcite cement and dolomite*

Mineral	Stage	Habit	Fe content
Calcite	1st	Fibrous at right angles to grain margin or syntaxial overgrowth parallel to c axis on echinoderm plates.	Poor.
	2d	Subequant independent of pore shape, obliterates all primary pore space.	Rich.
Dolomite	1st	Corroded grains or as "cloudy" cores to rhombs.	Rich.
	2d	External part of rhomb, free from inclusions, or as overgrowths on first-stage rhombs.	Poor.

ENVIRONMENTAL SIGNIFICANCE

Table 3 summarizes the preceding discussion and emphasizes the existence of at least two phases of formation of both sparry calcite cement and dolomite. The first phase of sparry calcite is free of iron, while the second stage is rich in iron; in contrast, the dolomite has a first phase that is rich in iron with an iron-poor second stage. Evamy (1969) has stated from the work of Castaño and Garrels (1950) and Garrels and Christ (1965) that ferrous iron is only stable during carbonate sedimentation under reducing conditions that occur dominantly below the water table. In addition, Evamy suggested that any ferrous iron incorporated into carbonate lattices beneath the water table is then stable through geological time. If this hypothesis is accepted, an environmental criterion can be established for ferroan calcites and dolomites, but, conversely, no criterion exists for interpreting the environmental formation of iron-free carbonate rocks. The environmental implications of the distribution of iron in the carbonate rocks of the Lisburne Group are:

1. The iron-poor calcite fringe cement was probably formed before the original aragonite of oolites or pelecypod fragments or the high-Mg calcite of echinoderm debris changed to stable low-Mg calcite. The fringe cement of the oolites and pelecypods probably has a common origin with the syntaxial overgrowths on echinoderm plates. It was suggested in the previous section that this iron-free first-phase cement originated by direct precipitation of $CaCO_3$ from supersaturated sea water.
2. The second-stage equant iron-rich pore-filling crystals of calcite (drusy-calcite of Bathurst, 1958) would, if the hypothesis of Evamy (1969) is accepted, be formed in the reducing environment beneath the water table, probably after the first-stage iron-rich dolomite. This sequence may indicate an external source of both calcium and carbonate ions, possibly $CaCO_3$-rich waters produced by the large-

scale solution of aragonitic components (as outlined by Bathurst, 1964, 1966).

The second-stage calcite cement ubiquitously fills the pore space in the Lisburne Group. To generate this vast amount of cement from internal sources, it would be necessary to dissolve a great quantity of aragonite. This process takes place preferentially in fresher waters (Cloud, 1962) and, as noted by Illing, Wood, and Fuller (1967, p. 498), could suggest that the Lisburne Group was deposited in an epicontinental sea of repeated uplift and downwarp.

3. The first-stage dolomite was rich in iron and commonly zoned (Katz, 1968). The original composition of dolomite is a function of the chemistry of the pore waters, and the zoning probably reflects their piecemeal formation. Commonly the iron-rimmed dolomites occur as clusters, the margins of which are abruptly terminated by the second-stage sparry calcite; the calcite having no relationship to the rhomb outlines. This fact suggests that the first-stage dolomite was formed from a local source (Murray, 1960) of magnesium ions as a replacement of original carbonate mud beneath the water table prior to introduction of the second-stage sparry calcite cement.
4. The second stage of dolomite formation probably represents replacement of calcite by the "distant sources" of magnesium (Murray, 1960). There is probably a time gap in the development of the second-stage dolomite after formation of the iron-rich core, but no criteria are available to suggest its duration. The absence of inclusions in the second-stage dolomite suggests that it formed by the physical creation of space during crystallization rather than by replacement.

CHERT

The structure of the abundant chert in the Lisburne Group is generally microscopically uniform, but from its original locus, two types can be distinguished—matrix (intergranular) chert and intragranular chert.

FABRIC

Matrix chert.—This chert tends to occupy the intergranular space between bioclasts, usually echinoderms or bryozoans, which are only marginally replaced (pl. 8, fig. 5). The blebs of matrix chert usually have an abrupt margin with the host limestone, but it is clear that the bedding is commonly displaced around the bleb, indicating either primary accumulation or postdepositional development prior to lithification. In contrast to the intragranular chert, the contained fragments of echinoderm debris show no evidence of concentration of silica within the plates.

Intragranular chert.—This chert type (fig. 20) is preferentially developed in echinoderm plates (pl. 9, figs. 1–6) or fibrous pelecypods (pl. 8, fig. 2). It occurs as a partial replacement or as preserved "ghost" structures.

Plate 10, figure 6, clearly shows the chert formed by the preferential replacement of the bioclastic debris of the Lisburne Group. In the upper part of the specimen, the crinoid fragments are yellow and stand out in relief above the calcareous but nonsiliceous matrix after acid etching. At the base of the core specimen, crinoid debris set in a similar matrix is preserved in sparry calcite.

Many echinoderm plates (pl. 9, figs. 1–6) and fibrous pelecypods are partly replaced by chert, yet other parts of the enclosing rock contain no silica whatsoever. A penumbra in which the pore structure of the echinoderm plate has been destroyed and which appear to be composed of an intimate admixture of silica and calcite commonly surrounds the silica blebs. The other grains are affected by the chertification only where the

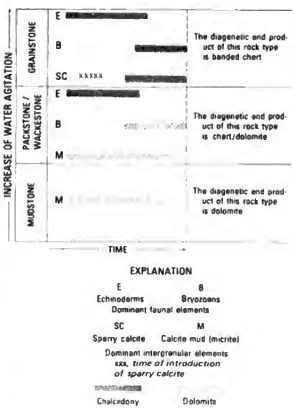

FIGURE 20.—Diagenetic history of limestones containing intragranular chert.

echinoderm plates and pelecypods are completely replaced. If the original interstitial material was sparry calcite cement, this cement is also eventually replaced by chert, but any original carbonate mud is preferentially replaced by dolomite rather than chert (pl. 8, figs. 7, 8).

TIME OF ORIGIN

The photomicrographs of plate 7 confirm the early diagenetic formation of intragranular chert and provide a framework from which a large part of the sequence of diagenesis of the Lisburne Group can be deciphered.

The single anhedral crystal of sparry calcite in the center of the field of view contains a line of micrite inclusions. This crystal is interpreted as an original echinoderm plate in which the original pore outlines are still preserved; the plate is bounded by the remains of a micrite envelope, and the whole is then encompassed by a syntaxial overgrowth. The micrite envelopes (pl. 9, figs. 3, 8) are common features on bioclasts and are believed to form immediately after death of the organism by the intersecting surface burrows of algae (Bathurst, 1966). At approximately this stage, silica began to nucleate in the pore space of the echinoderm plate and formed approximately equidimensional crystallites.

The first stage of sparry calcite then formed as a syntaxial overgrowth around the original echinoderm fragment, leaving a line of micrite inclusions as the only remnant of the micrite envelope. The absence of inclusions in the syntaxial overgrowth and the fracture of a bryozoan frond against an adjacent foraminifer suggest that this overgrowth was developed in a void with complementary pushing aside of any accessible carbonate grains or mud.

The next stage of diagenesis was the development of fibrous silica extending from the original spotted nucleus into the syntaxial overgrowth of sparry calcite. The final stage was the second phase of sparry calcite cementation with radiaxial and equant texture.

This sequence of diagenesis clearly demonstrates that the original silica nucleation within the echinoderm plates took place at a very early phase of diagenesis, probably before lithification. The extent of subsequent chertification is probably a function of the local availability of silica in the pore waters.

MODE OF ORIGIN

It is obvious that the intragranular cherts are formed by replacement of an original limestone with the silica first nucleating in the plates of echinoderms. However, the evidence for the origin of matrix chert is ambiguous; feasible hypotheses are: either preferential replacement of the matrix by silica or the presence of an original siliceous deposit.

If both the intragranular and matrix cherts originated by replacement of calcium carbonate by silica, it is difficult to reconcile both types being formed in the same depositional regime. Accepting the well-documented preferential replacement of echinoderm plates in the intragranular cherts, it is necessary to imply that the matrix chert was originally a primary deposit of biogenic origin. This kind of origin would then allow adjacent pore fluids to be strongly enriched in silica, which could then form intragranular cherts by replacement of bioclastic limestones.

SOURCE OF SILICA

Because of the low solubility of silica in sea water, the process of derivation of the opaline silica now forming vast thicknesses of chert and flint in the sedimentary column has been a matter of considerable argument.

It is widely accepted (MacKenzie and Garrels, 1966) that the bulk of the silica supplied to the oceans reacts with bicarbonate and other cations to form reconstituted clay minerals, thus maintaining a low concentration of silica in sea water. However, Calvert (1968) has made a convincing case for the primary biological control of the silica content of sea water, and he suggested that the reconstitution of clay minerals is probably a diagenetic reaction.

Diatoms, Radiolaria, and sponges are the main organisms with siliceous skeletons (Siever, 1957; Pittman, 1959). Krauskopf (1959) suggested that the siliceous skeletons of these organisms are protected by organic films which decompose after death and permit slow dissolution. Solution of the skeletons produces interstitial waters containing more than four times as much silica as normal sea water (Siever, 1959) and very close to saturation (Calvert, 1968). Interstitial waters of sediments from the South Pacific have been shown (Arrhenius, 1963) to have silica contents ranging from 6 to 788 ppm.

Calvert (1968) has shown that at the present day the Antarctic belt of siliceous oozes accounts for 80 percent of the current silica presently being removed from the oceans. He also suggested that the band of siliceous sediment in the subarctic Pacific was developed as a result of high biological productivity in an area of oceanic upwelling, rich in nutrients. The transfer of silica from water to newly deposited sediment is probably continuous, and opaline silica is released from the tests of siliceous organisms within the developing sedimentary accumulation. In spite of references in the literature to primary silica gels (Bissell, 1959; Maxwell and others, 1970, p. 442), there is no evidence for the presence of silica in any form other than undissociated monomeric silicic acid in true solution at normal pH (Krauskopf, 1959; Siever, 1959).

Thick cherts of Eocene age containing abundant radiolarian debris have been found by the Deep Sea Drilling Project throughout the North Atlantic (Peterson and others, 1970) and in the South Atlantic (Maxwell and others, 1970). Consolidated Eocene chert from Hole 8A of the Deep Sea Drilling Project on the northeast flank of the Bermuda Rise contains as much as 80 percent recognizable radiolarian remains (Wood, 1969). In contrast, Radiolaria are preserved as sparry calcite in lime mudstone in Hole 5A on the west flank of the Hatteras Abyssal Plain (Wood, 1970). The replacement of originally siliceous organisms by calcite, as also observed in the Cenomanian limestone of Lurestan, Iran, confirms that the silica of the original skeletons was released into the host sediment after deposition.

Ernst and Calvert (1969) described a stratigraphic sequence passing from diatomite to porcellanite to chert from top to base of the Monterey Formation of California, and they suggested that the silica has been progressively recrystallized down the section. The rate of recrystallization is considered to be relatively constant, and Ernst and Calvert showed that, in the presence of stagnant pure connate water, the Monterey porcellanite (cristobalite) should recrystallize to chert (quartz) in 180 million years. Mizutani (1970) confirmed this transition by experimental investigation under hydrothermal conditions.

The Eocene cherts of the Atlantic (Peterson and others, 1970, p. 422) are dominantly cristobalite in composition, and the radiolarian remains, as mentioned above, are well preserved. These rocks are approximately 50 million years old, and their mode of preservation would fit into the Ernst and Calvert hypothesis. The rare preservation of silica-bearing organisms in older cherts (especially those of Paleozoic and older age) is probably a function of their position at the end of the recrystallization sequence and in no way reflects an inorganic origin.

Evidence for the source of silica in the Lisburne Group is scanty, but examples of sponge spicules preserved in silica (pl. 8, fig. 1) or in calcite or dolomite (pl. 8, fig. 3) do exist. The specimens are composed of closely packed sponge debris, and similar accumulations could represent the local source of silica for the matrix chert. The common occurrence of cracks (pl. 9, fig. 5) within and surrounding the chert bodies can be attributed to the progressive desiccation of porcellanite.

The nucleation of the "intragranular chert" started, as has been previously mentioned, in the pore spaces of plates of echinoderms that were originally composed of a single crystal of high-Mg calcite (Donnay and Pawson, 1969). These plates have a spongelike internal structure so that only a small fraction of the plate volume is occupied by continuous crystalline calcite (Nissen, 1969). The spongelike internal structure is ramified with mesodermal tissue. Collagen fibers occur in the hollow spaces between the trabeculae of the echinoderm. It is possible that nucleation started in the spaces between the trabeculae as a result of reaction of calcite in the skeleton with complex organosilicic acids that were produced by the reaction of decomposing organic matter with pore waters heavily enriched in silica either from in situ release or from siliceous skeletons. In this way silica would be precipitated and replace calcite, probably on a molecular basis. However the silica concentration in the intragranular cherts took place, it certainly started prior to lithification just below the sediment-water interface and, probably, before the transition from the original high-Mg calcite skeleton to stable low-Mg calcite.

DOLOMITE IN CHERT

The presence of dolomite in chert has been recorded by many authors (for example, Pittman, 1959; Banks, 1970; Rapson-McGugan, 1970). Pittman (1959) suggested that this is evidence for postdolomite origin of the chert. He suggested that the dolomite was formed from the original limestone, the remains of which were subsequently replaced by silica. This explanation for the dolomite rhombs is not acceptable for the cherts of the Lisburne Group. Dolomite is sometimes present in chert when it is totally absent from the host limestone. Dolomite rhombs are often concentrated along the margins of the intragranular chert; these rhombs suggest that occurrence of dolomite in chert is a genetic association.

In some samples the dolomite in chert is euhedral (pl. 8, figs. 7, 8), while in others the rhombs are strongly corroded. The dolomites in the intragranular chert of crinoid plates (see above) are commonly rich in iron and concentrated along the edges of the chert, whereas in the matrix chert no iron enrichment was observed. Plate 9, figure 3, shows an example of the concentration of iron-rich dolomite at the edge of chert developed within a crinoid plate. The rhombs and patches of rhombs tend to be elongated parallel to the direction of cleavage of both the crinoid plate and its syntaxial overgrowth. The distribution of the dolomite can be related to that of a "reaction rim" in which the dolomite is a product of chert formation.

If organosilicic acids generated in the pores of both crinoid plates and fibrous pelecypods are responsible for the development of intragranular chert, as previously suggested, then the solution of calcium carbonate on a microscopic scale will result in simultaneous deposition of chert. The source of magnesium for the dolomite is almost certainly the high-Mg calcite of the original crinoid skeleton, but such impurities as iron are concen-

trated within the dolomite lattice. In the example illustrated on plate 9, figure 3, the presence of a "reaction rim" of iron-rich dolomite suggests that a process of progressive solution and reprecipitation of dolomite operates as the chert develops in the crinoid ossicle, but this process is by no means ubiquitous as evidenced by the homogeneous distribution of dolomite rhombs in some intragranular cherts. Organosilicic acids (Siever and Scott, 1963) can presumably dissolve calcite into solution but leave dolomite largely insoluble at the reaction interface. The restriction of dolomite to a reaction rim suggests that a local increase of acidity within earlier chert will lead to solution of early dolomite, which in turn will be reprecipitated at the chert-calcite margin.

SULFATES

Three sulfate minerals, anhydrite ($CaSO_4$), celestite ($SrSO_4$), and barite ($BaSO_4$), occur as rare accessories in the Lisburne Group of the subsurface, but none have been found in the surface outcrops of the Sadlerochit Mountains. This absence from the outcrops may well be a function of subaerial solution; nevertheless, no resultant casts have been recorded either in hand specimen or in thin section.

The distinction between these three minerals is often difficult in this section, all three crystallizing in the orthorhombic system. Anhydrite has the lowest relief and highest birefringence; the distinction between barite and celestite requires the use of an X-ray diffractometer or detailed refractive index measurements before positive identification is possible.

ANHYDRITE

Description.—Anhydrite occurs in cores from at least two wells about 1,500 feet beneath the top of the Lisburne Group. It occurs in two distinct habits, both associated with microdolomite. These are:

1. Nodules as much as 2 cm in diameter composed of felted prisms of anhydrite with a curvilinear orientation parallel to the outline of the nodule (pl. 11, fig. 4); and
2. Poikilotopic anhydrite (as much as 1 mm in diameter) enclosing abundant microdolomite.

Interpretation.—The crystal habits of the anhydrite are closely comparable with those described and illustrated by Wood and Wolfe (1969) from the Arab-Darb Formation of the Arabian Gulf. An arid supratidal (sabkha) origin has been suggested for the Arab-Darb Formation. Shearman (1966) regarded all nodular anhydrites as indicating formation within the capillary zone of arid supratidal environments. The poikilotopic anhydrite is considered by Wood and Wolfe to be of early secondary origin, and that it probably was formed by the enlargement of anhydrite cement between dolomite rhombs by the progressive replacement of the dolomite.

Plate II, figures 3 and 5, show two examples that suggest anhydrite has been taken into solution even in the subsurface. Figure 5 illustrates nodules in a laminated dolomite lined with a 1-mm layer of cryptocrystalline silica and largely filled with sparry calcite. The sparry calcite does not completely occupy the nodule. The preservation of good crystal terminations on the calcite suggests that the nodules were at one time voids subsequently infilled by both silica and calcite deposited from solution. The nodules probably were initially composed of anhydrite (cf. Wood and Wolfe, 1969, pl. 1). They evidently formed before the lithification of the rock, because the laminae above them are arched. The solution of the original anhydrite probably took place in interstratal solutions at an early stage of diagenesis.

Plate II, figure 3, shows a poikilotopic development of silica in dolomite whose external form is closely comparable with the poikilotopic anhydrite of Wood and Wolfe (see their plate IIIA); this form could also represent solution of an original anhydrite.

Armstrong, Mamet, and Dutro (1970) and Armstrong (1973) have recorded algal-mat dolomites comparable to that illustrated in plate 11, figure 5. These rocks occur in the Lisburne Group in the Sunset Pass section (68A–4A/4B), in the central Sadlerochit Mountains (68A–3), and in the Franklin Mountains (68A–1), about 870 feet, 650 feet, and 800 feet, respectively, beneath the top of the sections. An intertidal sabkha origin has been inferred for these rocks, and the discovery of sabkha-type anhydrites in the subsurface could support this conclusion.

CELESTITE

Description.—Celestite occurs abundantly in a 4-foot interval of core in one of the wells in which anhydrite has been observed and below the lowest record of anhydrite. Two of its distinct habits appear to be dependent on the nature of the host rock. These are:

1. Equigranular texture with partly interlocking crystals as much as 2 mm long. The celestite crystals are free from inclusions except for minute laths of anhydrite, the subparallel orientation of which ignores the orientation of the celestite. The host rock is a microdolomite (crystal size <5 μm) with scattered calcite crystals of similar size. Patches of the host contain relics after a pellet limestone, but the microdolomite between individual crystals of celestite parallels the crystal margin as though the celestite formed by pushing aside the host rock rather than by replacement. The anhydrite inclusions are probably a replace-

ment product after celestite—possibly in response to a slight prevailing stress, and

2. Partly dolomitized oolite pellet grainstone with the celestite occupying the intergranular spaces with poikilotopic or simple pore-fill textures (pl. II, fig. 2). The dolomite (individual crystals are <5μm) appears to be scattered through the clasts but is occasionally concentrated as fringes to them. The dolomitization certainly took place after the formation of the oolite skin but before cementation by celestite. In one specimen the oolite pellet grainstone has both celestite and calcite cement. Both minerals have a pore-fill texture, and from their relationship it is difficult to be certain which was deposited first, but an isolated example of a fringe of sparry calcite around a grain completely enclosed in celestite suggests that the calcite was the first to crystallize. Veinlets crosscut the rock, but their mineral filling faithfully reflects the nature of the immediate host.

Interpretation.—Many authors have recorded the presence of celestite in minor amounts in carbonate rocks (Deer and others, 1966). Evans and Shearman (1964) have described anhedral and "rosette" type celestite from modern algal-mat sediments of the Trucial Coast of Arabia. Kinsman (1969a) recorded that celestite is a fairly common early diagenetic minor mineral of coastal sabkhas and is most abundant in areas of intense dolomitization. In addition, Schmidt (1965) has described both replacement and cement celestite in the Gigas Beds of northwest Germany, the habits of which are closely comparable to those described from the Lisburne Group.

Recent work by Kinsman and Holland (1969) on the coprecipitation of strontium with aragonite has shown that the ratio of Sr^{+2}/Ca^{+2} in the aragonite (if other factors are equal) decreases with increasing temperature but is independent of the rate of precipitation. Kinsman (1969b) has also shown that skeletal aragonite can be distinguished from inorganic aragonite on the basis of the lower strontium content. For example, the Sr^{+2} content of coral aragonite in the Arabian Gulf is 7,740± 300 ppm (parts per million) while that of probable inorganic lagoonal aragonite muds is 9,390± 500 ppm.

The metastability of aragonite leads to its conversion to low-Mg calcite either by large-scale solution and precipitation that destroy the original texture of the aragonite grains or by piecemeal solution and immediate reprecipitation on a submicrometre scale that preserves the original texture. Stehli and Hower (1961) have shown the median Sr^{+2} content of Pleistocene calcite limestones of Florida is 1,100 ppm. Although Sr^{+2} concentrations show considerable variation in both calcite limestones and dolomites (<1,000 ppm Sr dolomites of the Trucial Coast sabkhas (Kinsman, 1969a)), the differences between these values and those of original aragonite are very high. These concentrations then provide pore waters with a high Sr^{+2}/Ca^{+2} ratio as demonstrated by Harriss and Matthews (1968) in the Pleistocene of Barbados. Kinsman (1969a) suggested that movement of diagenetic pore waters gives higher Sr^{+2} values in the downflow direction.

From this data we infer that the original aragonite of both the open-water and sabkha carbonate rocks may have been the source of the Sr^{+2}, and the excess SO_4^{-2} ions may have been provided during sabkha sedimentation. The downward migration of pore fluids would then provide a mechanism for their progressive enrichment in Sr^{+2} until a critical value was reached to allow formation of celestite.

BARITE

Barite has been recorded in only two samples of Lisburne Group rocks from the subsurface. The samples were taken within 6 feet of each other but in a well from which no sabkha-type sediments or other sulfate minerals have been recorded. The barite occurs in isolated clear porphyrotopes as much as 1 mm long in both pellet grainstone and an iron-rich wackestone (pl. 11, fig. 1). The euhedral shape of the crystals and the absence of inclusions suggest that the barite has, like celestite, formed by pushing aside the host rock rather than by replacement. Barite is often a product of low-temperature hydrothermal alteration (Dunham, 1934), but no evidence of this has been found in the Lisburne Group.

MARBLE

Recrystallization of sedimentary limestones (marbles) is defined by Spry (1969, p. 114) as "the reconstitution of an existing phase which may consist merely of an increase (grain-growth) or change in grain shape by grain boundary movement or by coalescence without nucleation." Recrystallized limestone—marble—is found in both the western Sadlerochit Mountains (69A–1) and Old Man Creek (69A–4/4K) sections interbedded with unaltered sedimentary limestones.

PURE CALCITE MARBLES

WESTERN SADLEROCHIT MOUNTAINS SECTION

In the western Sadlerochit Mountains section (69A–1), the marbles are found in the interval

1,080–1,140 feet (pl. 2, fig. 2; pl. 6, figs. 7, 8) in a discrete unit and at 1,015 and 998 feet as thin individual layers interbedded with unaltered fine-grained bioclastic pellet packstones. These marbles are composed exclusively of calcite. The individual anhedral grains show no sign of their origin, and the extensive interfingering of the grain margins has obliterated any intergranular space. The fabric can be referred to as "granoblastic-polygonal" (Spry, 1969, p. 187) and could be the product of posttectonic (annealing) crystallization (Turner and Weiss, 1963, p. 354–355).

Three main fabric types are traceable in the 69A–1 marble zone. These are, in probable order of formation:

1. Coarse grains of calcite with well-developed twinning that usually have corroded margins and often occupy the core of even larger unstrained calcite grains. The twinned grains are probably remnants of crinoid ossicles, as shown by the occasional preservation of the characteristic pore pattern upon which the twinning has been superimposed.
2. Clear untwinned equidimensional calcite that replaces the earlier twinned calcite. Extensive interpenetration of grain margins and lobate triple-point grain boundaries are common (Spry, 1969, p. 19); the grains intersect at approximately 120°.
3. Minute (~ 10μm) equidimensional calcite grains are distributed across both earlier fabrics but preferentially developed along grain margins.

Figure 21 shows the position of the various rock types within the interval 950–1,150 feet, section 69A–1, and the proportions of the various recrystallized fabric types are listed against the level of each marble sample. Over the section 1,080–1,140 feet, which is exclusively marble, the proportion of the latest granulation fabric type increases progressively toward +1,140 feet. The sedimentary limestones on either side of this zone show no effect of recrystallization.

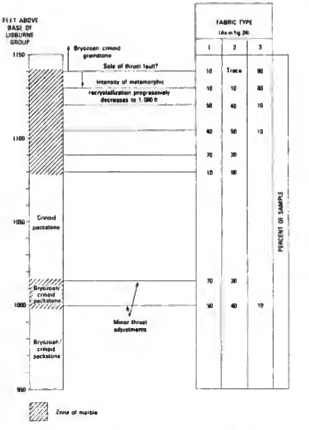

FIGURE 21.—Stratigraphic distribution of metamorphic fabrics in dynamically recrystallized limestones, western Sadlerochit Mountains section 69A–1. The columns at right show percentages of each of three fabric types developed in samples from various horizons in the Lisburne Group. See text for description of the fabric types.

OLD MAN CREEK SECTION

In the Old Man Creek (69A–4/4K) section (pl. 6, figs. 3–5), the modification of the original sedimentary limestone texture is not only more varied in its effect but also more extensive in its development. The total 1,500 feet of section exhibits some degree of fabric modification in the limestones, but the interbedded dolomites, apart from partial dedolomitization, appear unaffected. Not only are the three fabric types described from the western Sadlerochit Mountains section (69A–1) extensively represented but two additional types were noted. These are:

1. Strongly lineated rocks in which probable crinoid ossicles have been deformed into ellipses with an elongation ratio (a:b) of up to 4:1. Recrystallization is lacking; the intergranular material of packstones remains as carbonate mud. Thin discontinuous en echelon veinlets filled with sparry calcite are commonly superimposed upon this lineated fabric and intersect the lineation at up to 20°.
2. The twinning of originally untwinned crinoid ossicles and interpenetration of the margins with the intergranular sparry calcite cement.

MODE OF ORIGIN

The stratigraphic restriction of the marbles in the western Sadlerochit Mountains section (69A–1) and the large distance from the nearest known igneous mass (Mount Michelson is about 20 miles distant) makes metamorphism along a major bedding-plane thrust the

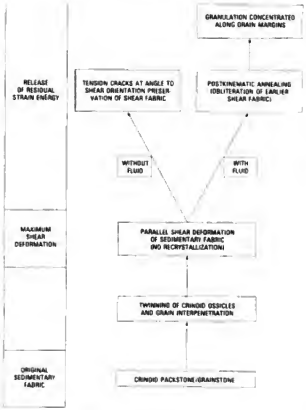

FIGURE 22.—Generalized sequence of dynamic metamorphism in limestones of the Lisburne Group.

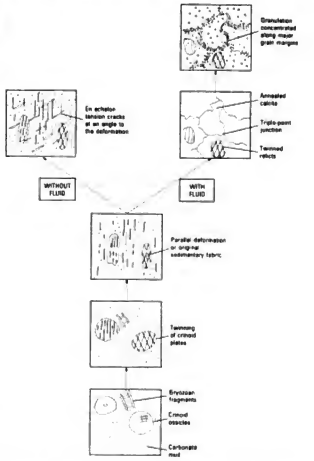

FIGURE 23.—Diagrammatic sequence of dynamic metamorphism in limestones of the Lisburne Group.

obvious mechanism to produce such extensive fabric alteration. No thrust was originally noted in the field, but in support of the thrusting hypothesis there is a marble unit (1,190 ft) that coincides with a marked break in the section (see figs. 2, 5) and this break has been suggested to be the contact between the Alapah and Wahoo Limestones. A study of the literature indicates that extensive production of marble along a thrust plane is not common, but Dr. Janet Watson of Imperial College, University of London, has suggested to us that a similar (but thinner) development occurs at the base of the Glaurus thrust in the Helvetic Alps of eastern Switzerland.

In spite of the differences between the fabric types in the recrystallized limestone of the western Sadlerochit Mountains (69A–1) and Old Man Creek (69A–4/4K) sections, it is possible to incorporate the differing fabrics into a single mechanism of origin (figs. 22–24). The first stage is the development of twinning in the coarse-grained element of the original sedimentary fabric, that is, the originally untwinned crinoid debris. The atomic rearrangement necessary in single calcite crystals for polysynthetic twinning is simple and can easily be induced artifically either by pressing a crystal with a knife in the appropriate direction (Spry, 1969, p. 85) or even during the preparation of a thin section (Dr. Janet Watson, oral commun., 1970). Griggs, Turner, and Heard (1960) produced twinning in single crystals of calcite by deformation. It is probable that twinning was superimposed on the coarser calcite crystals (either large crystals of sparry calcite cement or crinoid ossicles) at the first stage of deformation, and the results have only been preserved where the annealing recrystallization has not totally obliterated the early-stage fabric.

When the stress induced by thrust movement passes the appropriate plastic field to reach the fracture point for calcite, shearing produces parallel deformation of the original fabric and stretches the large grains. Upon reaching the fracture point, the free energy resulting from strain within the lattice is released by fracturing. The residual-strain energy is then gradually released and produces a significant temperature rise.

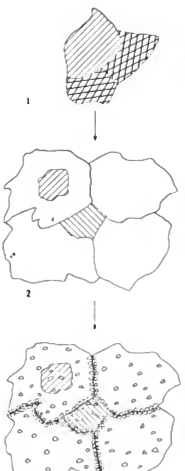

FIGURE 24.—Sequence of crystallization in marble of section 69A–1.

This residual-strain energy provides the mechanism for the strain-free annealing recrystallization, which results in the large untwinned crystals (often including relicts of twinned calcite) with approximately 120° triple-point junctions. The grain size of an annealed fabric increases with time and with rise in temperature (Turner and Weiss, 1963, p. 332). Griggs, Turner, and Heard (1960) have shown that for annealing in a low strain-stress field, recrystallization of Yule Marble was only partly complete at 800°C. This temperature, however, is not likely to be produced along a thrust plane. Buerger and Washken (1947) commented that a mineral will not recrystallize without solvents unless heated to a critical temperature. It would appear that to obtain the annealed fabrics observed in the Lisburne Group, extensive fluids must have been present after the thrusting episode. These fluids were probably acidic and occurred along the intergranular boundaries, which would allow piecemeal change of the fabric. Lack of annealing in the rarely preserved shear fabrics and associated on echelon tension gashes (especially in the Old Man Creek section) can be explained by the absence of postshearing fluids.

The final stage of recrystallization is represented by granulation of the annealed fabric mainly along grain margins but also within the grains themselves. This granulation is possibly a result of rotation of individual crystals. If this dynamic metamorphic sequence is realistic, then it appears that the metamorphism along the suggested thrust in 69A–1 is restricted to the sole and is absent from the thrust sheet itself.

The fabric changes in the Old Man Creek section (69A–4/4K) are much more extensive than those in the western Sadlerochit Mountains section (69A–1). The age of the Mount Michelson pluton is not certain (Leffingwell, 1919; Sable, 1965; Reiser, 1970). Although no fabric is definitely attributable to thermal alteration, it is possible that repeated shearing directly related to earth movements immediately prior to and associated with emplacement of the granite was the major mechanism of metamorphism. The extensive interfingering of grain margins in the rocks of the Old Man Creek section could be a reflection of thermal alteration. The preservation of shear fabrics in the Old Man Creek section suggests that interstitial fluids were localized, in contrast to the marbles of the western Sadlerochit Mountains section. This evidence would support a post-Pennsylvanian age for the Mount Michelson pluton.

DOLOMITES ASSOCIATED WITH MARBLE

Description.—An apparent anomaly in the Old Man Creek section is the absence of obvious stress response in the dolomite layers abundantly interbedded with the altered limestones. Two explanations are possible for this phenomenon—either (1) the time of dolomite formation was later than the shearing and subsequent annealing of the limestone, or (2) dolomite responds differently to shearing stress in that it can remain unaffected while calcite reaches its fracture point and becomes subsequently annealed (fig. 25).

The distribution of dolomite appears to be directly related to the original sedimentary fabric, and rhombs superimposed on a sheared or completely annealed limestone fabric have not been observed. Where dolomite is associated with marginally annealed limestones, the rhombs tend to be at least partly dedolomitized; they show corroded edges and internal spotty replacement by calcite. These facts suggest that the dolomite was formed before shearing occurred.

Mode of origin.—If, as suggested in the previous section, calcite and dolomite behave differently under

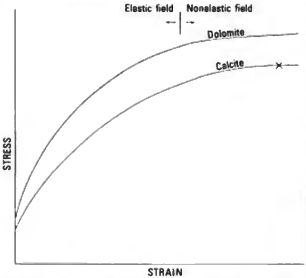

FIGURE 25.—Possible stress-strain relation of calcite and dolomite. Note that at a certain stress (x), calcite will fracture, whereas dolomite will still be in the elastic field.

shearing stress, a more detailed discussion of the relevant stress-strain curves is necessary.

Stress fields are expressed in terms of three vectors mutually at right angles and termed σ_1, σ_2, and σ_3 in decreasing order of magnitude (Mogi, 1971). In thrust faults the dominant direction of movement is horizontal with σ_1 and σ_2 in the horizontal plane and σ_3 vertical where $\sigma_1 > \sigma_2 > \sigma_3$. The elastic and plastic fields of deformation can be delimited on a stress-strain curve for a given mineral under constant temperature conditions. Mogi (1971) has shown that the stress-strain curves for calcite and dolomite diverge in a heterogeneous stress field, as they do in thrust faulting, with dolomite having a higher fracture point and greater ductility than calcite. Figure 25 indicates a possible stress-strain relation between calcite and dolomite which in thrust faulting would allow calcite to fracture while dolomite was still in the elastic field, as evidenced by the absence of flow or preferred orientation in the dolomite. This relationship could explain the apparent anomaly of limestones that exhibit strong deformation or annealing fabrics (interbedded) with apparently unaltered, but prekinematic, dolomites.

RELATIVE AGES OF FORMATION OF DIAGENETIC FEATURES

The preceding sections have presented the evidence and discussion for postdepositional alteration of the mineralogy and fabric in the Lisburne Group of the Sadlerochit Mountains. This section places these diagenetic phenomena into a time sequence and describes late-stage features formed as a result of overburden pressure or tectonic activity (the occurrence of marble having already been discussed). No attempt is made to reiterate the discussions of previous sections, and the conclusions are presented without further justification. It is often possible to assess the relative order of the start of development of the various diagenetic features, but comments on the relative time span or continuity of any process are usually conjectural.

1. The original nucleation of intragranular chert within crinoid plates and pelecypod fragments is considered to be the earliest phase of diagenetic alteration. Nucleation probably started immediately upon deposition prior to the conversion of original high-Mg crinoid debris or aragonitic pelecypod shells to stable low-Mg calcite. In the crinoids, dolomite formed as part of this silicification process from magnesium liberated from high-Mg calcite. This change was probably coincident with the development of micrite envelopes from marginal algal borings immediately upon death of the organism. Once nucleated, the chert developed gradually until at least after the second phase of calcite cementation has been completed.

   In contrast, the development of "matrix" chert is considered to be of direct biogenic origin, and its present-day fabric is related to its progressive recrystallization with time, generally producing a homogeneous texture that obliterates the original skeletons.

2. Closely following the nucleation of intragranular chert was the development of first-phase sparry calcite cement either as syntaxial overgrowths on the crinoid plates or as a fringe of fibrous crystals on carbonate clasts, such as oolites or pelecypods. The syntaxial overgrowths developed preferentially in the direction of the *c* axis (or axes) of the crinoid plates; these overgrowths acted as single crystals, by physically pushing aside rather than replacing any other carbonate debris. This first-phase cement in the Lisburne Group is everywhere poor in iron.

   High-Mg calcite debris probably lost its Mg^{2+} at this time, almost invariably on a piecemeal basis allowing the original fabric to be retained in low-Mg calcite.

   The change from aragonite to low-Mg calcite was generally later than the transformation of high-Mg calcite. Sometimes this change resulted from complete solution of aragonitic clasts. The micrite envelope and the first-phase sparry calcite fringe

provided a strong and probably elastic coating to the resulting void, which explains the scarcity of collapsed envelopes. The void was subsequently filled with equant sparry calcite, probably of the second phase, which obliterated the original internal fabric. When the test or skeleton was intimately intermixed with organic layers (as in fibrous pelecypods and oolites), the replacement took place as a result of small-scale solution of aragonite and almost simultaneous redeposition of low-Mg calcite. This process allowed the preservation of the original aragonitic fabric after transformation to calcite.

3. First-phase dolomite, the next new mineralogical form, developed into two distinct types. The first type was fine-grained dolomite that formed either as an early phase of sabkha (supratidal/intertidal) sedimentation from original carbonate mud or from the alteration of lagoonal carbonate muds. The fact that most of the dolomite is rich in iron may suggest that the Mg-rich waters that induced the alteration were derived from a reducing environment. Many of these dolomites were subjected to aggrading neomorphism that produced a fabric an order of magnitude coarser than when they were originally formed. Associated with the sabkha dolomites was the formation of anhydrite nodules and celestite. Some of these nodules have been replaced by calcite, probably during or after the development of second-phase sparry calcite cement.

   The second type of first-phase dolomite occurs as coarse rhombs, many larger than 200 micrometres, that developed in the grainstone facies and only partly replaced the clasts. These rhombs tend to be zoned as a result of variation in iron content; the zoning in turn reflects their piecemeal formation. The incorporation of iron into the dolomite lattice produced a nonstoichiometric mineral that appears to have been unstable and particularly prone to dedolomitization. Iron was commonly forced out of the dolomite lattice to form a rim around the rhomb now preserved as Fe_2O_3. These large rhombs often occur in intergranular clusters that are commonly crosscut by second-phase sparry calcite cement.

4. The fourth stage of diagenesis (coinciding with Stage IV of Land, 1967) was the formation of second-phase sparry calcite cement, which obliterated any pore space available in the limestones of the Lisburne Group. The cement occupies the intergranular space and fills the casts produced by solution of originally aragonitic bioclasts. The crystals tend to be subequant and become coarser toward the center of the void-fill. The presence of enfacial junctions between the first- and second-phase sparry calcite cements suggests a distinct time lapse between their formation. The second-phase sparry calcite, in contrast to the first phase, is often rich in iron; the addition of iron implies that fluids from which the cement was derived came from a "distant source."

5. The second phase of dolomite formation followed the introduction of the void-filling sparry calcite cement. Some of the macrodolomite in the Lisburne Group may have been developed during this phase of diagenesis, but the only positive evidence for its existence are the iron-free fringes of dolomite around the iron-oxide-rimmed first-phase dolomite and as an overgrowth that postdates the dedolomitization.

   Probably this phase is quantitatively of minor importance, but on its termination the rocks (except the marble) acquired the general fabric and mineralogy that have persisted until the present day. At this stage it is worth emphasizing that in the rocks in which intragranular chert has developed, the final rock type is a function of the nature of both the grains and the intragranular material (fig. 20). It must be emphasized, however, that the processes of alteration do not always go to completion.

   In grainstones, as chert developed in the crinoids, sparry calcite filled the intergranular space. As chert developed around the original nuclei, the other debris, the Bryozoa (mainly) and the sparry calcite cement, were eventually replaced, and the diagenetic end product is banded chert.

   In packstones and wackestones in which the intergranular spaces were originally filled with carbonate mud, chert developed in the crinoid debris, but the carbonate mud was preferentially dolomitized. The chert tended to be restricted to the crinoids, but dolomite replaced all the carbonate mud and the bryozoan debris as well. The diagenetic end product is an admixture of chert and dolomite.

   In mudstones where recognizable fossil debris is less than 10 percent, the carbonate mud was replaced by dolomite with no accessory minerals.

6. The first late-stage diagenetic features were stylolites, interfingering planes that almost certainly formed by solution as a response to overburden pressure. The minimum amount of solution that took place along any stylolite can be estimated from the amplitude of interfingering. Dunnington (1967) suggested that stylolites develop under at least 2,500 feet of overburden in the Dukhan Field

of Qatar. Stylolites are rare in thin sections of Lisburne Group rocks examined for this study, but it must be remembered that only a very small proportion of the total section was sampled, even though samples were taken at 5- to 10-foot intervals. The locus of stylolite development probably was preferentially determined by thin clay horizons. Plate 12, figure 2, illustrates a Lisburne Group stylolite with an amplitude of 0.5–1.5 mm whose plane is filled with bitumen and clay containing dolomite rhombs. Dolomite is absent from the adjacent host rock, so the rhombs in the stylolite probably were produced by very late stage Mg-rich solutions passing along the plane of the stylolite.

7. The final stages of diagenesis were associated with tectonic activity. Marble developed along the sole of bedding-plane thrusts, and intensive fractures, many filled with late-sparry calcite, transected all other features of the Lisburne Group (pl. 6, figs. 3–7).

SELECTED BIBLIOGRAPHY

Adams, J. E., and Rhodes, M. L., 1960, Dolomitization by seepage refluxion: Am. Assoc. Petroleum Geologists Bull., v. 44, p. 1912–1920

Alderman, A. R., and Skinner, H. C. W., 1957, Dolomite sedimentation in the South-East of South Australia: Am. Jour. Sci., v. 255, p. 561–567.

Armstrong, A. K., 1967, Biostratigraphy and carbonate facies of the Mississippian Arroyo Penasco Formation, north-central New Mexico: New Mexico Bur. Mines and Mineral Resources Mem. 20, 80 p., 10 pls., 45 figs.

———1970a, Carbonate facies and the lithostrotionid corals of the Mississippian Kogruk Formation, De Long Mountains, northwestern Alaska: U.S. Geol. Survey Prof. Paper 664, 38 p., 14 pls., 37 figs.

———1970b, Mississippian dolomites from Lisburne Group, Killik River, Mount Bupto Region, Brooks Range, Alaska: Am. Assoc. Petroleum Geologists Bull., v. 54, no. 2, p. 251–264, 10 figs.

———1972, Biostratigraphy of Mississippian lithostrotionoid corals, Lisburne Group, Arctic Alaska: U.S. Geol. Survey Prof. Paper 743–A, 55 p., 9 pls., 25 figs.

———1973, Pennsylvanian carbonate rocks, paleoecology, and colonial corals, north flank, eastern Brooks Range, Arctic Alaska: U.S. Geol. Survey Prof. Paper 747, 45 p., 7 pls., 16 figs.

———1974, Carboniferous carbonate depositional models, preliminary lithofacies and paleotectonic maps, arctic Alaska: Am. Assoc. Petroleum Geologists Bull., v. 58, no. 4, p. 621–645, 20 figs.

Armstrong, A. K., and Mamet, B. L., 1970, Biostratigraphy and dolomite porosity trends of the Lisburne Group, *in* Adkison, W. L., and Brosgé, M. M., eds., Proceedings of the geological seminar on the North Slope of Alaska: Los Angeles, Pacific Sec. Am. Assoc. Petroleum Geologists, p. N1–N16, 12 figs.

Armstrong, A. K., Mamet, B. L., and Dutro, J. T., Jr., 1970, Foraminiferal zonation and carbonate facies of the Mississippian and Pennsylvanian Lisburne Group, central and eastern Brooks Range, Alaska: Am. Assoc. Petroleum Geologists Bull., v. 54, no. 5, p. 687–698, 4 figs.

———1971, Lisburne Group, Cape Lewis-Niak Creek, northwestern Alaska, *in* Geological Survey research 1971: U.S. Geol. Survey Prof. Paper 750–B, p. B23–B34, 9 figs.

Arrhenius, G., 1963, Pelagic sediments, *in* Hill, M. N., ed., The Sea: New York, Interscience, v. 3, p. 692–727.

Banks, N. G., 1970, Nature and origin of early and late cherts in the Leadville Limestone, Colorado: Geol. Soc. America Bull., v. 81, p. 3033–3048.

Bathurst, R. G. C., 1958, Diagenetic fabrics in some British Dinantian Limestones: Liverpool and Manchester Geol. Jour., v. 2, p. 11–36.

———1959, Diagenesis in Mississippian calcilutites and pseudobrecias: Jour. Sed. Petrology, v. 29, p. 365–376.

———1964, The replacement of aragonite by calcite in the molluscan shell wall, *in* Imbrie, J., and Newell, N. D., eds., Approaches to Paleoecology: New York, Wiley and Sons, p. 356–376.

———1966, Boring algae, micrite envelopes, and lithification of molluscan biosparites: Geol. Jour., v. 5, p. 15–32.

———1971, Carbonate sediments and their diagenesis, Developments in Sedimentology No. 12: Amsterdam, Elsevier Publishing Co., 620 p.

Bausch, W. M., 1965, Dedolomitisierung und recalcitisierung in frankischen Malmkalken: Neues Jahrb. Mineralogie Monatsh., v. 3, p. 75–82.

Bissell, H. J., 1959, Silica in sediments of the Upper Paleozoic of the Cordilleran area, *in* Ireland, H. A., ed., Silica in Sediments: Soc. Econ. Paleontologists and Mineralogists Spec. Pub. 7, p. 150–185.

Blow, W. H., and Brooks, J., 1975, A model for the biochemical mechanisms of calcification in the Globigerinacea, *in* The Cainozoic Globigerinida, Part II, Danian to Oligocene Planktonic Foraminiferal Biostratigraphy: Leiden, Brill (in press).

Bowsher, A. L., and Dutro, J. T., Jr., 1957, The Paleozoic section in the Shainin Lake area, central Brooks Range, Alaska: U.S. Geol. Survey Prof. Paper 303–A, 39 p., 6 pls., 4 figs.

Braun, M., and Friedman, G. M., 1970, Dedolomitization fabric in peels: a possible clue to unconformity surfaces: Jour. Sed. Petrology, v. 40, no. 1, p. 417–419.

Brosgé, W. P., Dutro, J. T., Jr., Mangus, M. D., and Reiser, H. N., 1962, Paleozoic sequence in eastern Brooks Range, Alaska: Am. Assoc. Petroleum Geologists Bull., v. 46, no. 12, p. 2174–2198.

Buerger, M. J., and Washken, E., 1947, Metamorphism of minerals: Am. Mineralogist, v. 32, p. 296–308.

Calvert, S. E., 1968, Silica balance in the ocean and diagenesis: Nature, v. 219, no. 5157, p. 919–920.

Castaño, J. R., and Garrels, R. M., 1950, Experiments on the deposition of iron with special reference to the Clinton iron ore deposits: Econ. Geology, v. 45, p. 755–770.

Chave, K. E., 1954, Aspects of the biogeochemistry of magnesium, 1, Calcareous marine organisms: Jour. Geology, v. 62, p. 266–283.

Chave, K. E., and Suess, E., 1967, Suspended minerals in sea water: New York Acad. Sci. Trans., ser. II, v. 29, p. 991–1000.

Cloud, P. E., Jr., 1962, Environment of calcium carbonate deposition west of Andros Island, Bahamas: U.S. Geol. Survey Prof. Paper 350, p. 1–138.

Collier, A. J., 1906, Geology and coal resources of the Cape Lisburne region, Alaska: U.S. Geol. Survey Bull. 278, 54 p.

Davies, G. R., 1970, Carbonate bank sedimentation, Eastern Shark Bay, Western Australia, *in* Carbonate sedimentation and environment, Shark Bay, Western Australia: Am. Assoc. Petroleum Geologists Mem. 13, p. 85–168.

Deer, W. A., Howie, R. A., and Zussman, J., 1966, An introduction to the rock forming minerals: London, Longmans, 528 p.

Deffeyes, K. S., Lucia, F. J., and Weyl, P. K., 1965, Dolomitization of Recent and Plio-Pleistocene sediments by marine evaporite waters on Bonaire, Netherlands Antilles, *in* Pray, L. C., and Murray, R. C., eds., Dolomitization and limestone diagenesis; a sym-

posium: Soc. Econ. Paleontologists and Mineralogists Spec. Pub. 13, p. 71–88.

De Groot, K., 1967, Experimental dedolomitization: Jour. Sed. Petrology, v. 37, p. 1216–1220.

Detterman, R. L., 1970, Sedimentary history of the Salderochit and Shublik Formations in northeastern Alaska, *in* Adkison, W. L. and Brosgé, M. M., eds., Proceedings of the geological seminar on the North Slope of Alaska: Los Angeles, Pacific Sec. Am. Assoc. Petroleum Geologists, p. O1–O13, 9 figs.

Donahue, J., 1965, Laboratory growth of pisolite grains: Jour. Sed. Petrology, v. 35, p. 251–256.

Donnay, G., and Pawson, D. L., 1969, X-ray diffraction studies of echinoderm plates: Science, v. 166, p. 1147–1150.

Duck, E. W., 1966, Emulsion polymeriaation, *in* Encyclopedia of Polymer Science and Technology: New York, Interscience, v. 5, p. 801–859.

Dunham K.C., 1934, The genesis of the North Pennine ore deposits: Geol. Soc. London Quart. Jour., v. 90, p.689–717.

Dunham, R. J., 1962, Classification of carbonate rocks according to deposition texture, *in* Classification of carbonate rocks—A symposium: Am. Assoc. Petroleum Geologists Mem. 1, p. 108–121.

———1969, Early vadose silta in Townsend Mound (Reef), New Mexico, *in* Friedman, G. M., ed., Depositional environments in carbonate rocks; a symposium: Soc. Econ. Paleontologists and Mineralogists Spec. Pub. 14, p. 139–181.

Dunnington, H. V., 1967, Aspects of diagenesis and shape change in stylolitic limestone reservoirs: World Petroleum Cong., 7th, Mexico City 1967, Proc., v. 2, p. 339–352.

Dutro, J. T., Jr., 1970, Pre-Carboniferous carbonate rocks, northeastern Alaska, *in* Adkison, W. L., and Brosgé, M. M., eds., Proceedings of the geological seminar on the North Slope of Alaska: Los Angeles, Pacific Sec. Am. Assoc. Petroleum Geologists, p. M1–M7.

Dutro, J. T., Jr., Brosgé, W. P., and Reiser, H. N., 1972, Significance of recently discovered Cambrian fossils and reinterpretation of Neruokpuk Formation, northeastern Alaska: Am. Assoc. Petroleum Geologists, v. 56, no. 4, p. 808–815, 4 figs.

Ernst, W. G., and Calvert, S. E., 1969, An experimental study of the recrystallization of porcellanite and its bearing on the origin of some bedded cherts: Am. Jour. Sci., Schairer Volume. v. 267–A, p. 114–133.

Evamy, B. D., 1963, The application of a chemical staining technique to a study of dedolomitization: Sedimentology, v. 2, p. 164–170.

———1967, Dedolomitization and the development of rhombohedral pores in limestones: Jour. Sed. Petrology, v. 37, p. 1204–1215.

———1969, The precipitational environment and correlation of some calcite cements deduced from artificial staining: Jour. Sed. Petrology, v. 38, no. 3, p. 787–793.

Evamy, B. D., and Shearman, D. J., 1965, The development of overgrowths from echinoderm fragments: Sedimentology, v. 5, p. 211–233.

———1969, Early stages in development of overgrowths on echinoderm fragments in limestones: Sedimentology, v. 12, p. 317–322.

Evans, G., and Shearman, D. J., 1964, Recent celestite from the sediments of the Trucial Coast of the Persian Gulf: Nature, v. 202, p. 385.

Folk, R. L., 1959, Practical petrographic classification of limestones: Am. Assoc. Petroleum Geologists Bull., v. 43, p. 1–38.

———1965, Some aspects of recrystallization in ancient limestones, *in* Pray, L. C., and Murray, R. C., eds., Dolomitization and limestone dingenesis: a symposium: Soc. Econ. Paleontologists and Mineralogists Spec. Pub. 13, p. 14–48.

Freeman, T., 1971, Morphology and composition of Ordovician vadose cement: Nature (Physical Science), v. 233, p. 133–134.

Friedman, G. M., 1959, Identification of carbonate minerals by staining methods: Jour. Sed. Petrology, v. 29, p. 87–97.

Friedman, G. M., and Sanders, J. E., 1967, Origin and occurrence of dolostones, *in* Chilingar, G. V., Bissell, H. J., and Fairbridge, R. W., eds., Carbonate rocks: origin, occurrence and classification: Amsterdam, Elsevier Publishing Co., p. 267–348.

Fritz, P., 1967, Oxygen and carbon isotopic composition of carbonates from the Jura of Southern Germany: Canadian Jour. Earth Sci., v. 4, p. 1247–1267.

Garrels, R. M., and Christ, C. L., 1965, Solutions, minerals, and equilibria: New York, Harper and Row, 450 p.

Goldsmith, J. R., and Graf, D. L., 1958, Structural and compositional variations in some natural dolomites: Jour. Geol., v. 66, p. 678–693.

Griggs, D. T., Turner, F. J., and Heard, H. C., 1960, Deformation of rocks at 500°C to 800°C: Geol. Soc. America Mem. 79, p. 39–104.

Harris, W. H., and Matthews, R. K., 1968, Subaerial diagenesis of carbonate sediments: efficiency of the solution-precipitation process: Science, v. 160, p. 77–79.

Henbest, L. G., 1968, Diagenesis of oolitic limestones of Morrow (Early Pennsylvanian) age in northwestern Arkansas and adjacent Oklahoma: U.S. Geol. Survey Prof. Paper 594–H, 22 p.

Illing, L. V., Wells, A. J., and Taylor, J. C. M., 1965, Penecontemporary dolomite in the Persian Gulf, *in* Pray, L. C., and Murray, R. C., eds., Dolomitization and limestone diagenesis: a symposium: Soc. Econ. Paleontologists and Mineralogists Spec. Pub. 13, p. 89–111.

Illing, L. V., Wood, G. V., and Fuller, J. G. C. M., 1967, Reservoir rocks and stratigraphic traps in non-reef carbonates: World Petroleum Cong., 7th, Mexico City 1967, Proc., v. 2, p. 487–499.

Katz, A., 1968, Calcian dolomites and dedolomitization: Nature, v. 217, no. 5127, p. 439–440.

———1971, Zoned dolomite crystals: Jour. Geology, v. 79, p. 38–51.

Kendall, C. G. St. C., and Skipwith, P. A. d'E., 1969, Holocene shallow-water carbonate and evaporite sediments of Khor al Bazam, Abu Dhabi, southwest Persian Gulf: Am. Assoc. Petroleum Geologists Bull., v. 53, p. 841–869.

Kinsman, D. J. J., 1966, Gypsum and anhydrite of recent age, Trucial Coast, Persian Gulf, Symposium on Salt: Northern Ohio Geol. Soc., 2d, Cleveland, Ohio 1966, p. 302–326.

———1969a, Modes of formation, sedimentary associations, and diagnostic features of shallow-water and supratidal evaporites: Am. Assoc. Petroleum Geologists Bull., v. 53, no. 4, p. 830–840, 3 figs.

———1969b, Interpretation of Sr^{2+} concentrations in carbonate minerals and rocks: Jour. Sed. Petrology, v. 39, p. 486–508.

Kinsman, D. J. J., and Holland, H. D., 1969, The co-precipitation of cations with CaCO₃. IV. The co-precipitation of Sr^{2+} with aragonite between 16° and 96° C: Geochim. et Cosmochim. Acta, v. 33, p. 1–17.

Kitano, Y., and Hood, D. W., 1965, The influence of organic material on the polymorphic crystallization of calcium carbonate: Geochim. et Cosmochim. Acta, v. 29, p. 29–41.

Krauskopf, K. B., 1959, The geochemistry of silica in sedimentary environments, *in* Ireland, H. A., ed., Silica in sediments: Soc. Econ. Paleontologists and Mineralogists Spec. Pub. 7, p. 4–19.

Krynine, P. D., 1948, The megascopic study and field classification of sedimentary rocks: Jour. Geology, v. 56, no. 2, p. 130–165.

Krynine, P. D., and Folk, R. L., 1950, Petrology of the Lisburne Limestone: U.S. Geol. Survey Inv. Naval Petroleum Reserve No. 4, Spec. Rept. 22, 25 p.

Krynine, P. D., Folk, R. L., and Rosenfeld, M. A., 1950, Porosity and petrology of Lisburne limestone samples from the Kanayut, Nanushuk, and Ikkilfik Lakes areas, with discussion of the distribution of porous zones in the Lisburne limestone by Arthur L.

Bowsher, Sr.: U.S. Geol. Survey Inv. Naval Petroleum Reserve No. 4, Spec. Rept. 17, 18 p.

Land, L. S., 1967, Diagenesis of skeletal carbonates: Jour. Sed. Petrology, v. 37, p. 914–930.

——1971, Submarine lithification of Jamaican Reefs, *in* Carbonate cements: Bricker, O.P., ed., Johns Hopkins Univ. Studies Geology, no. 19, p. 59–71.

Land, L. S., Mackenzie, F. T., and Gould, S. J., 1967, Pleistocene history of Bermuda: Geol. Soc. America Bull., v. 78, p. 993–1006.

Leffingwell, E. de K., 1919, The Canning River region, Northern Alaska: U.S. Geol. Survey Prof. Paper 109, 251 p.

Logan, B. W., Read, J. F., and Davies, G. R., 1970, History of carbonate sedimentation, Western Australia, *in* Carbonate sedimentation and environments, Shark Bay, Western Australia: Am. Assoc. Petroleum Geologists Mem. 13, p. 38–84.

Lucia, F. J., and Murray, R. C., 1967, Origin and distribution of porosity in crinoidal rock: World Petroleum Cong., 7th, Mexico City 1967, Proc., v. 2, p. 409–423.

Mackenzie, F. T., and Garrels, R. M., 1966, Silica-bicarbonate balance in the oceans and early diagenesis: Jour. Sed. Petrology, v. 36, no. 4, p. 1075–1084.

Mamet, B. L., and Armstrong, A. K., 1972, Lisburne Group, Franklin and Romanzof Mountains, northeastern Alaska, *in* Geological Survey research 1972: U.S. Geol. Survey Prof. Paper 800-C, p. C127–C144, 10 figs.

Martin, A. J., 1970, Structure and tectonic history of the western Brooks Range, De Long Mountains and Lisburne Hills, northern Alaska: Geol. Soc. America Bull., v. 81, p. 3605–3622, 7 figs.

Mattavelli, L., Chilingarian, G. V., and Storer, D., 1969, Petrography and diagenesis of the Taormina Formation, Gela oil field, Sicily: Sed. Geology, v. 3, p. 59–86.

Maxwell, A. E., and others, 1970, Initial reports of the Deep Sea Drilling Project, Volume III: Washington, U.S. Govt. Printing Office, 806 p.

Mitterer, R. M., 1971, Influence of natural organic matter on CaCO$_3$ precipitation, *in* Bricker, O.P., ed., Carbonate cements: Johns Hopkins Studies Geology, no. 19, p. 252–258.

Mizuntani, S., 1970, Silica minerals in the early stage of diagenesis: Sedimentology, v. 15, p. 414–436.

Mogi, K., 1971, Effect of the triaxial stress system on the failure of dolomite and limestone: Tectonophysics, v. 11, p. 111–127.

Morlot, A. von, 1848, Sur l'origine de la dolomie (Extr. d'une letter de M. A. de Morlot à M. Elie de Beaumont): Acad. Sci. Paris Comptes Rendus, v. 26, p. 311–315 (*in* Cayeux, S., 1935, Les roches sédimentaires de France—Roche carbonatées: Paris, Masson et Cie, 447 p.).

Müller, G., and Tietz, G., 1971, Dolomite replacing "Cement A" in biocalcarenites from Fuerteventura, Canary Islands, Spain, *in* Bricker, O.P., ed., Carbonate cements: Johns Hopkins Univ. Studies Geology, no. 19, p. 327–329.

Murray, R. C., 1960, Origin of porosity in carbonate rocks: Jour. Sed. Petrology, v. 30, p. 59–84.

——1964, Preservation of primary structures and fabrics in dolomite, *in* Imbrie, J., and Newell, N. D., eds., Approaches to Paleoecology: New York, Wiley and Sons, p. 388–403.

Murray, R. C., and Lucia, F. J., 1967, Cause and control of dolomite distribution by rock selectivity: Geol. Soc. America Bull., v. 78, p. 21–36.

Newell, N. D., Purdy, E. G., and Imbrie, J., 1960, Bahamian oolitic sand: Jour. Geology, v. 68, p. 481–497.

Nissen, H. V., 1963, Röntgengefügeanalyse am Kalzit von Echinodermenskeletten: Neues Jahrb. Geologie Paläontologie Abh., v. 117, p. 230–234.

——1969, Crystal orientation and plate structure in echinoid skeletal units: Science, v. 166, p. 1150–1152.

Oldershaw, A. E., and Scoffin, T. P., 1967, The source of ferroan and non-ferroan calcite cements in the Halkin and Wenlock Limestones: Geol. Jour., v. 5, p. 309–320.

Peterson, M. N. A., and others, 1970, Initial reports of the Deep Sea Drilling Project, Volume II: Washington, U.S. Govt. Printing Office, 491 p.

Pittman, J. S., Jr., 1959, Silica in Edwards Limestone, Travis County, Texas, *in* Ireland, H.A., ed., Silica in sediments: Soc. Econ. Paleontologists and Mineralogists Spec. Pub. 7, 121–134.

Pray, L. C., and Choquette, P. W., 1966, Genesis of carbonate reservoir facies [abs.]: Am. Assoc. Petroleum Geologists Bull., v. 50, p. 632.

Purdy, E. G., 1968, Carbonate diagenesis: an environmental survey: Estratto da Geologica Romana, v. 7, p. 183–228.

Purser, B. H., 1969, Syn-sedimentary marine lithification of middle Jurassic limestones in the Paris Basin: Sedimentology, v. 12, p. 205–230.

Rapson-McGugan, J. E., 1970, The diagenesis and depositional environment of the Permian Ranger Canyon and Mowitch Formations, Ishbel Group, from the southern Canadian Rocky Mountains: Sedimentology, v. 15, p. 363–417.

Reiser, H. N., 1970, Northeastern Brooks Range—a surface expression of the Prudhoe Bay section, in Adkison, W. L., and Brosgé, M. M., eds., Proceedings of the geological seminar on the North Slope of Alaska: Los Angeles, Pacific Sec. Am. Assoc. Petroleum Geologists, p. K1–K14.

Reiser, H. N., Brosgé, W. P., Dutro, J. T., Jr., and Detterman, R. L., 1971, Preliminary geologic map, Mt. Michelson quadrangle, Alaska: U.S. Geol. Survey open-file map, scale 1:250,000.

Reiser, H. N., Dutro, J. T., Jr., Brosgé, W. P., Armstrong, A. K., and Detterman, R. L., 1970, Progress map, geology of the Sadlerochit and Shublik Mountains [Alaska]: U.S. Geol. Survey open-file map, scale 1:63,360.

Sable, E. G., 1965, Geology of the Romanzov Mountains, Brooks Range, Northeastern Alaska: U.S. Geol. Survey open-file report, 218 p.

Sandberg, P. A., 1971, Scanning electron microscopy of cheilostome bryozoan skeletons: techniques and preliminary observations: Micropaleontology, v. 17, p. 129–151.

Schmidt, V., 1965, Facies, diagenesis and related reservoir properties in the Gigas Beds (Upper Jurassic), Northwestern Germany, *in* Pray, L. C., and Murray, R. C., eds., Dolomitization and limestone diagenesis: a symposium: Soc. Econ. Paleontologists and Mineralogists Spec. Pub. 13, p. 124–168.

Scholle, P. A., 1971, Sedimentology of fine-grained deep-water carbonate turbidites, Monte Antola flysch (Upper Cretaceous), Northern Appenines, Italy: Geol. Soc. America Bull., v. 82, p. 629–658.

Schrader, F. C., 1902, Geologic section of the Rocky Mountains in northern Alaska: Geol. Soc. America Bull., v. 13, p. 233–252.

Schroeder, J. H., Dwornik, E. J., and Papike, J. J., 1969, Primary protodolomite in echinoid skeletons: Geol. Soc. America Bull., v. 80, p. 1613–1616.

Shearman, D. J., Khouri, J., and Taha, S., 1961, On the replacement of dolomite by calcite in some Mesozoic limestones from the French Jura: Geologists' Assoc. Proc., v. 72, p. 1–12.

Shearman, D. J., Twyman, J., and Zand Karimi, M., 1970, The genesis and diagenesis of oolites: Geologists' Assoc. Proc., v. 81, p. 561–575.

Shinn, E. A., 1969, Submarine lithification of Holocene carbonate sediments in the Persian Gulf: Sedimentology, v. 12, p. 109–144.

Siever, R., 1957, The silica budget in the sedimentary cycle: Am Mineralogist, v. 42, pts. 11–12, p. 821–841.

——1959, Petrology and geochemistry of silica cementation in some Pennsylvanian sandstones, *in* Silica in sediments: Soc. Econ. Paleontologists and Mineralogists Spec. Pub. 7, p. 55–79.

Siever, R., and Scott, R. A., 1963, Organic geochemistry of silica, *in*

Ireland, H. A., ed., Organic Geochemistry: London, Pergamon Press, p. 579–595.

Simkiss, K., 1964, Variations in the crystalline form of calcium carbonate precipitated from artificial sea water: Nature, v. 201, p. 492–493.

Sorby, H. C., 1879, The structure and origin of limestones: Geol. Soc. London Proc., v. 35, p. 56–95.

Spry, A., 1969, Metamorphic textures: London, Pergamon Press, 350 p.

Stehli, F. G., and Hower, J., 1961, Mineralogy and early diagenesis of carbonate sediments: Jour. Sed. Petrology, v. 31, p. 358–371.

Tatarskiy, V. B., 1949, Distribution of rocks in which dolomite is replaced by calcite: Akad. Nauk S.S.S.R. Doklady.

Taylor, J. M. C., and Illing, L. V., 1969, Holocene intertidal calcium carbonate cementation, Qatar, Persian Gulf: Sedimentology, v. 12, p. 69–107.

Tillman, R. W., 1971, Petrology and paleoenvironments, Robinson Member, Minturn Formation (Desmoinesian), Eagle Basin, Colorado: Am. Assoc. Petroleum Geologists Bull., v. 55, p. 593–620.

Turner, F. J., and Weiss, L. E., 1963, Structural analysis of metamorphic tectonites: New York, McGraw Hill, 545 p.

Twyman, J. P., 1970, Recent oolites of the Trucial Coast, Arabian Gulf: London, England, University of London, Ph. D. thesis.

Wilbur, K. M., and Simkiss, K., 1968, Calcified Shells: Comprehensive Biochemistry, v. 26A, p. 229–295.

Wilson, J. L., 1970, Depositional facies across carbonate shelf margins: Gulf Coast Assoc. Geol. Socs. Trans., v. 20, p. 229–233.

———1974, Characteristics of carbonate-platform margins: Am. Assoc. Petroleum Geologists Bull., v. 48, no. 5, p. 810–824, 6 figs.

Winland, H. D., 1968, The role of high Mg calcite in the preservation of micrite envelopes and textural features of aragonite sediments: Jour. Sed. Petrology, v. 38, no. 4, p. 1320–1325.

———1971, Diagenesis of carbonate grains in marine and meteoric waters: Providence, R. I., Brown University, Ph. D. thesis, 320 p.

Wolfe, M. J., 1968, Lithification of a carbonate mud; Senonian chalk in Northern Ireland: Sed. Geology, v. 2, p. 263–290.

Wood, G. V., 1969, Sediment thin section data, Leg 1, Deep Sea Drilling Project, *in* Ewing, M., and others, Initial reports of the Deep Sea Drilling Project, Volume I: Washington, U.S. Govt. Printing Office, p. 348–353.

———1970, Sediment thin section data, Leg 2, Deep Sea Drilling Project, *in* Peterson, M. N. A., and others, Initial reports of the Deep Sea Drilling Project, Volume II: Washington, U.S. Govt. Printing Office, p. 323–328.

Wood, G. V., and Wolfe, M. J., 1969, Sabkha cycles in the Arab/Darb Formation off the Trucial Coast of Arabia: Sedimentology, v. 12, p. 165–191.

INDEX

[Italic page numbers indicate major references]

☆ U.S. GOVERNMENT PRINTING OFFICE : 1975 O – 573-516

PLATES 1–12

PLATE 1

FIGURE 1. Oolitic bioclastic grainstone, 70A–5, 1,988 feet, ×65. Thin oolitic skins show both radial and concentric structure around bioclasts, some of which are crinoid debris. In contrast to figure 3, however, the less equant debris has no oolitic coating. Two phases of cement are present.

2. Oolitic grainstone, 69A–1, 1,385 feet ×65. Thin oolitic skins developed around bioclastic cores of diverse shapes. The cores range from equidimensional crinoid plates to bryozoan clasts to elongate pelecypod fragments. The intergranular space has been filled with sparry calcite.

3. Oolitic grainstone, 69A–1, 340 feet, ×65. The oolitic coatings developed around nuclei of either crinoid or bryozoan clasts. The foraminifer on the left of the field has no oolitic coating. Two generations of sparry calcite cement are shown. The first, a fibrous coating perpendicular to the edges of the oolite grains, is iron-free calcite; the second, occupies the intergranular pore space, is equant iron-rich calcite crystals.

4. Oolitic packstone and grainstone, 68A–4A, 1,180 feet, ×65. The skin of the central oolite is displaced from the original core. The outer part of the core was presumably dissolved, after which the iron-poor first-phase sparry calcite cement was deposited with a radial fabric on the inner surface of the oolitic coating. A fracture then transected the lower part of the oolite and caused the oolitic skin to be partly ripped away from the core. The remainder of the original core space and the new void caused by the movement of the oolite skin away from the core were then filled with iron-rich second-phase sparry calcite cement.

5. Oolitic grainstone, 68A–4A, 1,090 feet, ×65. Developement of thin oolitic coatings with radial texture around irregular pellet and bioclastic debris. Two phases of sparry calcite cement are clearly distinguishable—first, an iron-free fringe around the grains, and second, an iron-rich phase filling the intergranular spaces.

6. Bioclastic grainstone with pelecypods and bryozoans, 70A–5, 1,910 feet, ×33. Fragment of pelecypod shell with internal divisions preserved by micritic partitions at right angles to the shell wall. The outline of the shell is preserved by a micrite envelope. Two generations of sparry calcite are observable. In the first phase, a thin layer of prismatic calcite probably grew to the outer shell wall that was originally aragonite; the calcite and the micrite envelope gave the shell sufficient rigidity to withstand compaction when the original aragonite wall dissolved.
The second-phase cement may have entered the cast by the upper break in the skeleton wall (boring?) and, in the left hand part of the skeleton, appears to have displaced the partitions from the upper shell wall. The second-phase cement has equant crystals that transect the shell partitions.

7. Bryozoan crinoid grainstone, 70A–5, 2,450 feet, ×33. Hexagonal syntaxial overgrowth of sparry calcite on crinoid plate. Lines of inclusions show the progressive development of the overgrowth.

8. Bryozoan crinoid grainstone, 70A–5, 2,430 feet, ×33. Echinoderm spine set in a sparry calcite cement. Probable micrite envelope. The microstructure of the spine has been preserved (see left of field).

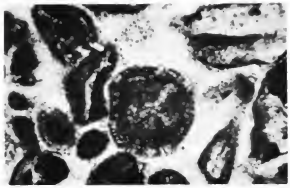

1

2

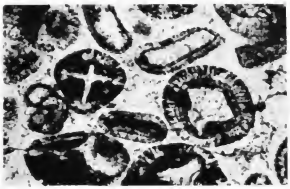

3

4

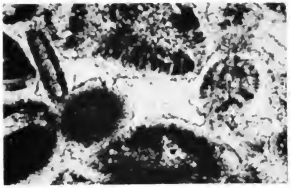

5

6

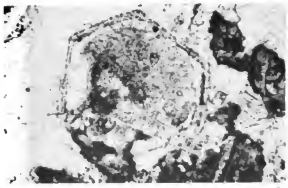

7

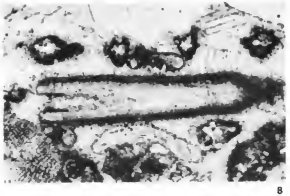

8

OOLITE BIOCLASTIC GRAINSTONE, OOLITIC GRAINSTONES, OOLITIC PACKSTONE/GRAINSTONE, BIOCLASTIC GRAINSTONE, AND BRYOZOAN CRINOID GRAINSTONES

PLATE 2

FIGURE 1. Bryozoan grainstone, 70A–5, 2,465 feet, ×33. The zooecia (cavities) of bryozoan fronds are completely filled with sparry calcite.

2. Bryozoan grainstone, 70A–5, 2,070 feet, ×33. Well-packed assemblage of elongate bryozoan fronds whose zooecia are filled with sparry calcite cement.

3. Dolomitic bryozoan grainstone, 68A–4A, 1,260 feet, ×65. The bryozoan zooecia are filled with carbonate mud in which dolomite rhombs are developed. A pelecypod cast (lower right) has been enclosed by a micrite envelope and adjacent to the shell wall the internal texture of the sparry calcite is prismatic and becomes equant in the center. This texture is typical of deposition from solution.

4. Bryozoan grainstone, 69A–1, 1,182 feet, ×65. Large fragment of a bryozoan frond in which the acanthoporee (interwall spaces) are filled with sparry calcite cement but the zooecia are lined with carbonate mud with a central development of sparry calcite, probably of neomorphic origin. The fabric of the sparry calcite in the zooecia has possibly been affected by the organic matter originally occupying this space.

5. Microdolomite, 70A–5, 2,090 feet, ×65. Bryozoan fragment set in a microdolomite host. The zooecia are filled with sparry calcite. The microdolomite is probably of very early diagenetic origin but has not replaced the bryozoan fragment to any extent.

6. Bioclastic microdolomite, 68A–4A, 1,100 feet, ×65. Individual rhombs of dolomite are stained by iron oxide. The dolomite almost certainly replaces original calcite mud but also fills bryozoan zooecia and marginally replaces the bioclastic skeletons.

7. Dolomitic crinoid bryozoan packstone, 68A–4A, 940 feet, ×33. Rhombs of dolomite (≈100μm) restricted to the carbonate mud matrix and outlined by iron oxides.

8. Dolomitic bryozoan packstone, 69A–1, 797 feet, ×100. Bryozoan fronds filled with carbonate mud in which dolomite rhombs are developed. Individual rhombs contain an iron-oxide zone toward the outer margin parallel to the rhomb faces. The dolomite is iron poor.

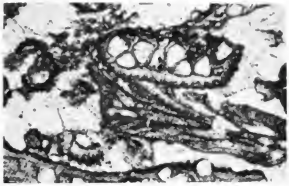

1

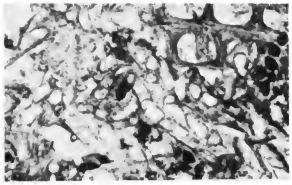

2

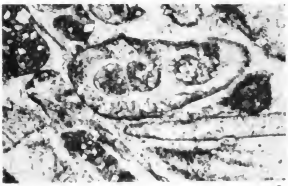

3

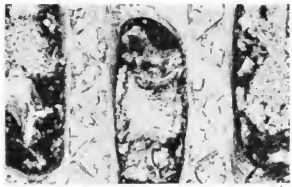

4

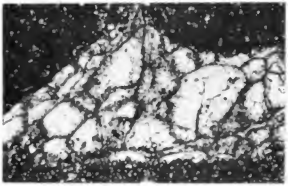

5

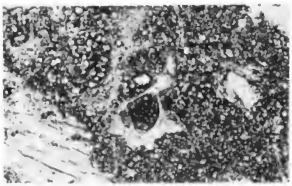

6

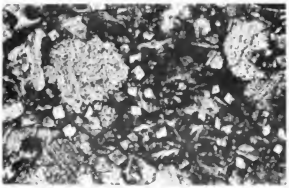

7

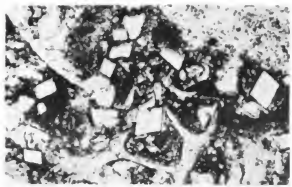

8

BRYOZOAN GRAINSTONES. DOLOMITIC BRYOZOAN GRAINSTONES, MICRODOLOMITE, BIOCLASTIC MICRODOLOMITE, DOLOMITIC CRINOID BRYOZOAN PACKSTONE, AND DOLOMITIC BRYOZOAN PACKSTONE

PLATE 3

FIGURE 1. Bioclastic grainstone, 69A–4, 1160 ft, ×65. Bryozoan fragments set in sparry calcite. Original dolomite partly replaced by calcite in rhombs outlined by iron oxides.

2. Macrodolomite, 69A–4, 940 ft, ×65. Macrodolomite with yellow (phosphatic?) cores, and compound vein with coarsely crystalline dolomite at the center and quartz on the edges. This sample suggests that a fracture first was filled with quartz and upon later dilation was filled with dolomite.

3. Macrodolomite, 70A–4, 15 ft, ×65. Anhedral macrodolomite with intergranular hematitic clay.

4. Macrodolomite, crossed nicols, 69A–4K, 145 ft beneath base of Lisburne Group, ×80. Anhedral grains of macrodolomite with no intergranular porosity.

5. Microdolomite, subsurface, ×50. A bryozoan (stained by Alizarin Red S) set in a matrix of microdolomite. The zooecia of the bryozoan are largely filled with dolomite and the external margins are partly replaced. Traces of unreplaced bryozoa that are scattered throughout the dolomite demonstrate large-scale replacement of skeletal matter.

6. Macrodolomite, 70A–4, 720 feet, ×65. Anhedral macrodolomite with iron-rich cores (stained by potassium ferricyanide) and later iron-free rims.

7. Macrodolomite, 70A–4, 125 feet, ×65. Macrodolomite rhombs with cloudy cores and clear rims. The cores tend to be iron rich and the rims iron poor.

8. Microdolomite with clot of iron oxide, 69A–1, 593 feet, ×65. In the bulk of the rock individual rhombs are zoned with a cloudy iron-rich core and an iron-poor outer zone. In contrast, the rhombs within the clot have an internal zone of iron oxide parallel to the rhombic faces, and the dolomite is iron poor. The iron oxides in the clot may have originated from an original unstable iron-rich dolomite, whereas outside the clot the iron-rich dolomite core has remained stable and iron oxides are absent. The outer iron-free dolomite appears to be a ubiquitous later phase in both the clot and the host rock.

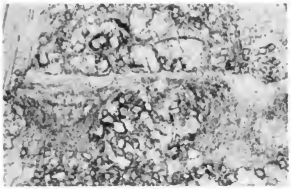

1

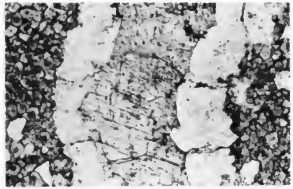

2

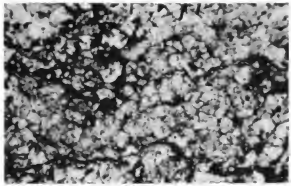

3

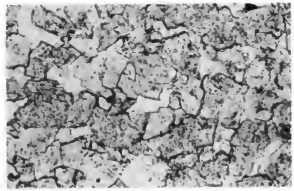

4

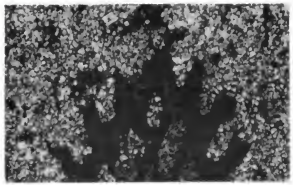

5

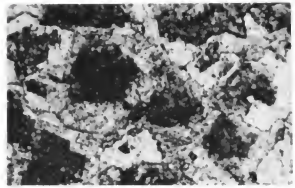

6

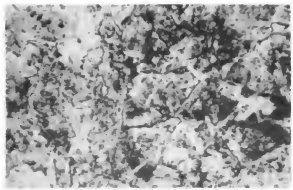

7

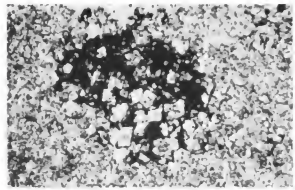

8

BIOCLASTIC GRAINSTONE, MACRODOLOMITE, MICRODOLOMITE, MICRODOLOMITE WITH CLOT OF IRON OXIDE

PLATE 4

FIGURE 1. Macrodolomite, 69A–1, 375 ft, ×65. Zoned rhombs of macrodolomite with interrhombic iron oxide.

2 Iron-rich dolomite, 69A–1, 60 feet, ×33. Typical view illustrating crosscutting relation between sparry calcite cement (above) and earlier dolomite. In the center of the field is a dolomite rhomb with a dedolomitized zone of calcite parallel to the rhomb faces, and immediately below is an iron-rich dolomite with no apparent zonation. This whole zone of early dolomite is rich in iron oxide.

3, 6. Dolomitic bioclastic grainstone, 69A–1, 455 feet, ×65. Rhombs of iron-poor dolomite edged with iron oxide. A thin zone of calcite is developed toward the outer edges of the rhombs and parallel to the rhomb faces. Inner parts of rhombs are commonly void, probably because of postdedolomitization solution.

4. Bioclastic grainstone, 69A–1, 330 feet, ×65. The bioclasts have a thin patina (replacive?) of dolomite (shown as a white rim) formed before the sparry calcite cement.

5. Dolomitic bioclastic grainstone, 69A–1, 465 feet, ×65. Scattered intergranular dolomite rhombs, each of which is rimmed by iron oxide. Calcite zones near the outer edges and parallel to the rhomb faces were produced by dedolomitization. Centers of rhombs are either void or contain partly dissolved dolomite.

7. Dedolomite, 69A–4, 330 feet, ×80. Corroded macrodolomite rhomb with outer dark zone replaced by sparry calcite. A calcite-filled veinlet partly transects the rhomb.

8. Early dolomite, 69A–1, 60 feet, ×33. Iron-rich dolomite and partly dedolomitized rhombs surrounded by later sparry calcite cement. The margins of the dolomite are surrounded by pyrite that probably formed as a residue after the replacement of iron-rich dolomite by calcite.

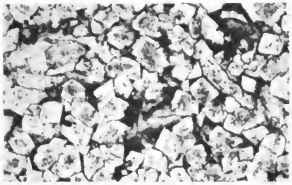

1

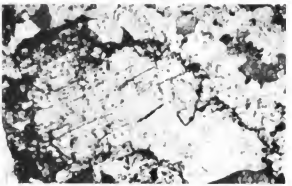

2

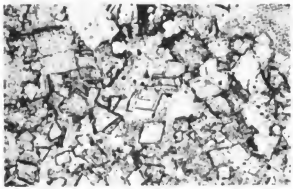

3

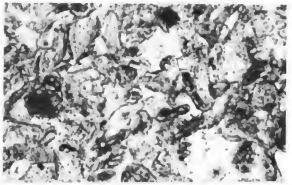

4

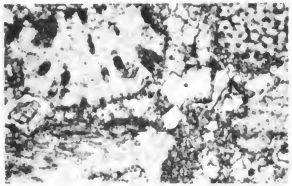

5

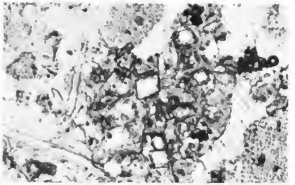

6

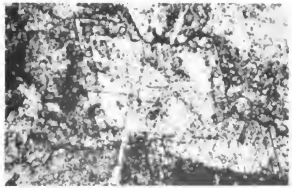

7

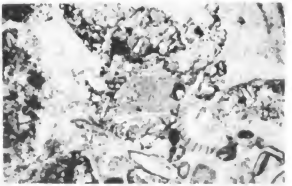

8

MACRODOLOMITE, IRON-RICH DOLOMITE, DOLOMITIC BIOCLASTIC GRAINSTONE, DEDOLOMITE, EARLY DOLOMITE

PLATE 5

[All samples from 69A-1, 60 ft]

FIGURE 1. ×32, plane-polarized light. Stained by Alizarin Red S. Rhombs of dolomite set in sparry calcite cement. The white zones parallel to the original rhomb faces are calcite (dedolomite). Overgrowths of homogeneous dolomite occur in two stages parallel to the line of intersection of the rhomb faces. Hematite is developed in patches, some at the edge of the original rhomb and included within the overgrowth, and others on the outer edges of the overgrowths.

2. ×32, crossed nicols. Stained by Alizarin Red S. Same field as above. The original rhomb extinguishes in quadrants in continuity with the adjacent dolomite overgrowth. The dedolomitized calcite zones are of different optical orientation than the surrounding dolomite.

3. Interpretation of the field represented by 1 and 2 above. The optical continuity of the dolomite overgrowth with the adjacent quadrant of the original dolomite rhomb but which is independent of the orientation of the dedolomitized zones of calcite is considered evidence that dedolomitization took place prior to the overgrowth.

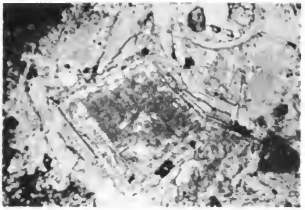

1

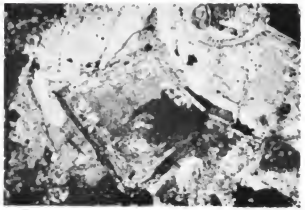

2

3

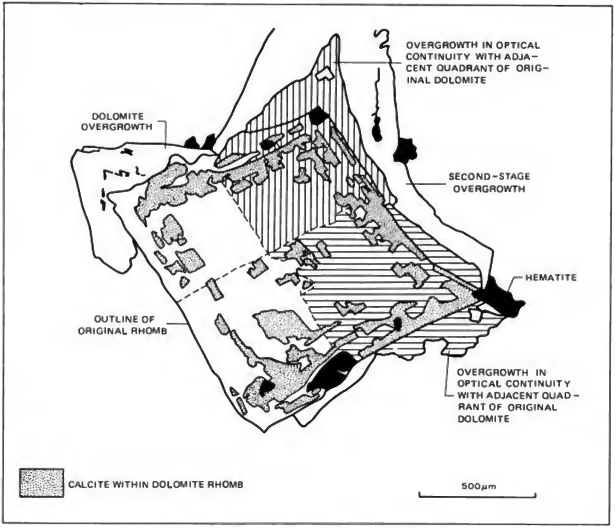

DEDOLOMITE WITH ANNOTATED DIAGRAM

PLATE 6

FIGURE 1. Bioclastic mudstone, 69A–1, 390 feet, ×65. Crinoid plate set in fine-grained matrix of calcite microspar. In the center of the field a crinoid plate has undergone grain diminution, especially the original outline and in a central "channel." Adjacent to the right side of the original crinoid plate is clear sparry calcite that probably represents a relic of the original syntaxial overgrowth.

2. Pellet intraclast grainstone, 70A–5, 2,045 feet, ×65. A high proportion of the grains show heterogeneous internal texture, and at first glance they might be interpreted as either reworked carbonate mud or pellets of fecal origin. In the center of the field, however, a crinoid plate shows marginal grain diminution, which may account for the origin of other grains (for example, the pellets or intraclasts) where the process of grain diminution has gone to completion. Two phases of sparry calcite can be observed.
3. Sheared limestone, 69A–4, 1,200 feet, ×65. Strong parallel lineation of sparry calcite pods and micrite. This structure almost certainly originated from shearing, but evidence of annealing is absent. Stylolites in this rock are superimposed on the shear fabric. Sparry calcite veinlets transect the shear fabric at 70°.
4. Shear fabric, marble, 69A–4, 1,190 feet, ×65. Shear fabric interrupted by a series of transverse displacements, in a sparry calrite crystal (probably originally a crinoid plate).
5. Sheared limestone, 69A–4K, 90 feet below base of Lisburne Group, ×65. Sheared limestone with argillaceous laminae and scattered coarse pods of sparry calcite.
6. Marble, 69A–1, 1,015 feet, ×65. Large dusty twinned calcite crystals replaced by a later stage undeformed clear calcite crystal. The margins of individual crystals are crenulated. The clear crystal is probably a product of annealing metamorphism.
7. Marble, 69A–1, 1,090 feet, ×33. Early twinned calcite, later untwinned calcite probably formed by annealing, and minor grain diminution along the crystal boundaries.
8. Marble, 69A–1, +1,130 feet, ×33. Large untwinned crystals of calcite of probable annealed origin with extensive interpenetration of grain margins and grain diminution concentrated along the major grain boundaries.

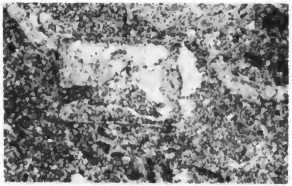

1

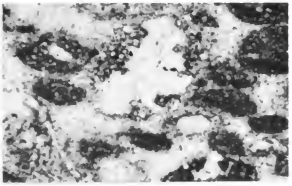

2

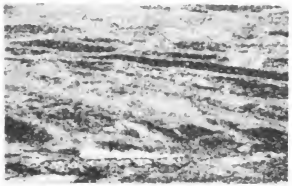

3

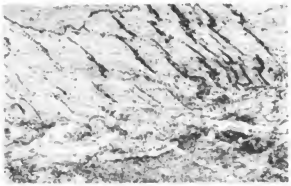

4

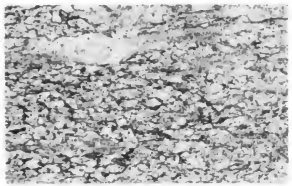

5

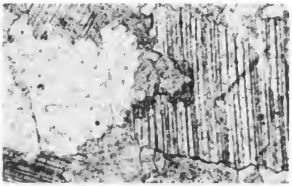

6

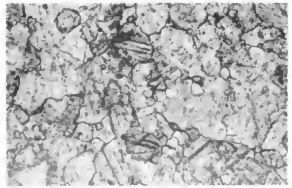

7

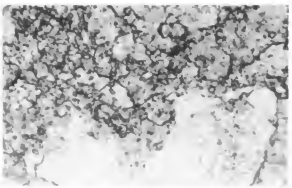

8

BIOCLASTIC MUDSTONE, PELLET INTRACLAST GRAINSTONE, SHEARED LIMESTONE, SHEAR FABRIC, MARBLE

PLATE 7

FIGURES 1–3. Sequence of diagenetic events ×50 subsurface. 1, Plane-polarized light; 2, Crossed nicols; 3, Interpretation. For discussion see section on "Time of Origin."

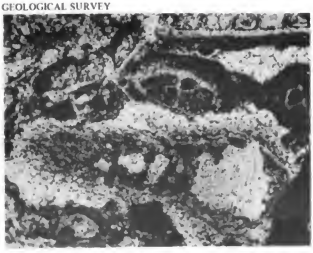

1

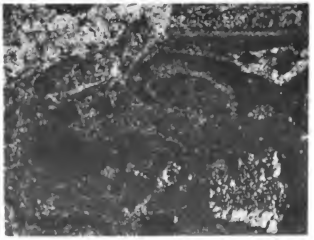

2

3

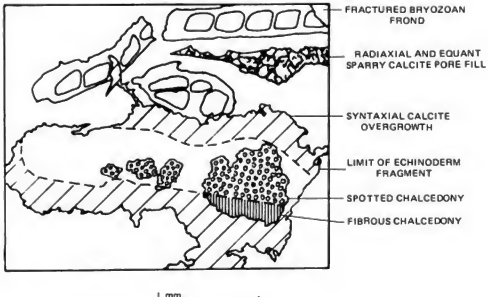

SEQUENCE OF DIAGENETIC EVENTS

PLATE 8

FIGURE 1. Chert, 69A–4, 340 ft, ×80. Chert with ghosts after sponge spicules.

2. Siliceous lime-mudstone, 69A–1, 15 feet below base of Lisburne Group crossed nicols, ×65. Casts after pelecypods infilled with chert showing early radial and final equant fabric that probably indicate deposition from solution.

3. Microdolomite, 70A–4, 1,130 feet, ×33. Sponge spicules preserved in chert set in a matrix of microdolomite.

4. Bryozoan crinoid packstone and grainstone, 68A–4A, 990 feet, ×33. The bryozoan zooecia (cavities) are patchily filled with and replaced by chert. The sparry calcite that also fills parts of the cavities is enriched in iron probably scavenged from the replaced calcite.

5. Calcareous chert, 69A–1, 350 feet, ×33. Bioclasts of bryozoan and crinoid debris set in a matrix of chert. Marginal replacement of the bioclasts is evident but no intragranular chert was recorded in this specimen.

6. Matrix chert, 68A–4B, 90 feet, ×33. Matrix chert with intense marginal corrosion of the included bioclasts.

7. Chert, 70A–4, 1,340 feet, ×80. Euhedral and partly corroded dolomite rhombs set in chert that is cut by a series of subparallel cracks.

8. Chert, 70A–4, 1,185 feet, ×33. Chert containing euhedral and corroded macrodolomite.

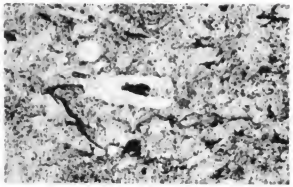

1

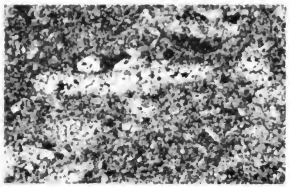

2

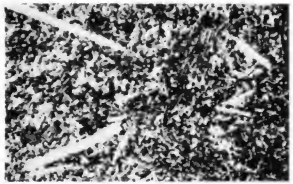

3

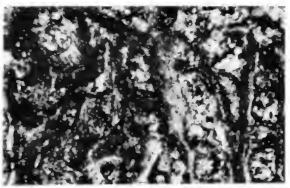

4

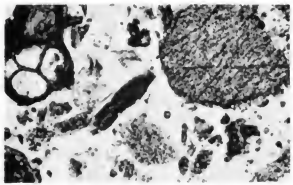

5

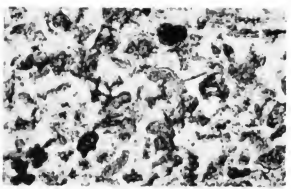

6

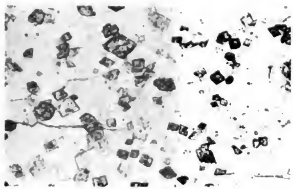

7

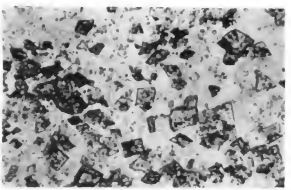

8

CHERT, SILICEOUS LIME-MUDSTONE, MICRODOLOMITE, BRYOZOAN CRINOID PACKSTONE/GRAINSTONE, CALCAREOUS CHERT, MATRIX CHERT, CHERT

PLATE 9

FIGURE 1. Bioclastic wackestone, 69A-1, 1,305 feet, ×65. Chert developed within a twinned crinoid plate and its overgrowth, both set in a carbonate mud matrix.

2. Crinoid bryozoan grainstone, 68A-4A, 950 feet, ×33. Chert nucleus that developed within crinoid ossicle and obliterated the pore pattern. The central canal of the ossicle is still visible (just above center of right edge of field). The sparry calcite surrounding the ossicle is a good example of a syntaxial overgrowth.

3. Bioclastic microdolomite, 68A-4A, 1,100 feet, ×65. Crinoid plate with intragranular development of chert set in microdolomite. Iron-rich macrodolomite rhombs developed at the chert-calcite interface.

4. Bryozoan crinoid packstone, 68A-4A, 1,625 feet, ×33. Crinoid plate with syntaxial overgrowth of sparry calcite and a patch of intragranular chert. A reaction rim of iron-rich dolomite occurs within the chert at the chert-calcite interface.

5. Bioclastic packstone, 69A-1, 1,352 feet, ×65. Pelecypod fragment now almost completely internally replaced by intragranular chert. The original curved growth-pattern of the pelecypod is preserved in the chert. The crack on the right side of the photograph is restricted to the chert and is probably a result of dehydration of porcellanite.

6. Bioclastic packstone, 69A-1, 1,320 feet, ×65. Intragranular chert developed in crinoid plate with well-preserved pore pattern. Carbonate mud matrix.

7. Dedolomite, 70A-4, 1,080 feet, ×100. Intergranular rhombs in a crinoid packstone. The large central rhomb is only marginally replaced by calcite, but the rhomb to the right and the corroded grain above center have been completely replaced by fine-grained calcite.

8. Bioclastic grainstone, subsurface, ×50. Crinoid plate with well-developed micrite envelope. Foraminifera (left) and Bryozoa (right) also present. First- and second-stage sparry calcite cement are well developed. Within the crinoid plate are chert patches surrounded by pin-point aureoles of chert in calcite (only noticeable under crossed nicols).

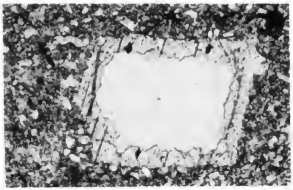

1

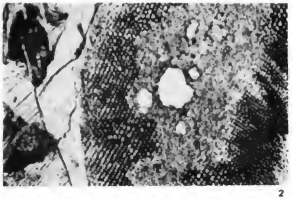

2

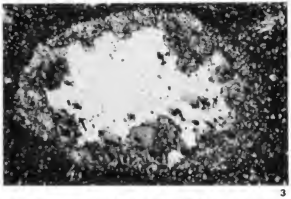

3

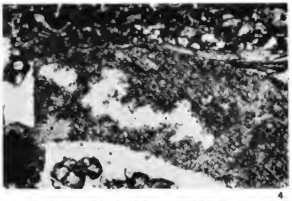

4

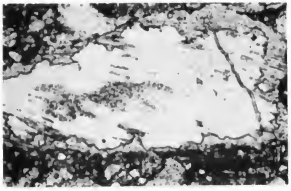

5

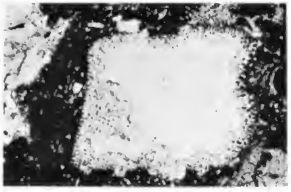

6

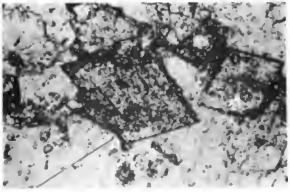

7

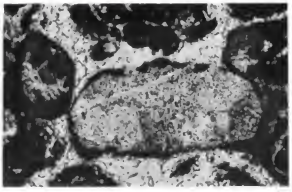

8

BIOCLASTIC WACKESTONE, CRINOID BRYOZOAN GRAINSTONE, BIOCLASTIC MICRODOLOMITE, BRYOZOAN CRINOID PACKSTONE, BIOCLASTIC PACKSTONE, DEDOLOMITE, BIOCLASTIC GRAINSTONE

PLATE 10

FIGURE 1. Chert and dolomite, subsurface, ×50. Ghost structures of crinoid fragments in chert set in a matrix of microdolomite. Preservation of traces of original pores of crinoid plates is particularly noteworthy.

2. Chert and dolomite, subsurface, ×50. Ghost structures of mollusk and crinoid fragments developed in chert and set in a matrix of microdolomite. The rock fabric suggests that this rock was originally a bioclastic packstone in which the bioclasts have been largely replaced by chert while the intergranular calcite mud has been replaced by dolomite.

3. *"Osagia"* grainstone, 68A–4A, 1,570 feet, ×65. Crinoid plate forms nucleus for *"Osagia."* Individual cusplike growth forms now preserved in chert.

4. *"Osagia"* grainstone, 68A–4A, 1,580 feet, ×65. Bryozoan fragment forms nucleus for an *"Osagia"* grain. Cusplike growth forms of *"Osagia"* now largely preserved in chert.

5. *"Osagia"* grainstone, subsurface, ×65. Compound grains of *"Osagia"* developed around a bioclastic core and set in a sparry calcite cement. The cement has an iron-poor fringe and a later iron-rich pore fill.

6. Argillaceous limestone, subsurface. A variegated bioturbated wackestone and packstone. Crinoid debris is abundant, preserved in chert at the top of the specimen and preserved in calcite at the base. Except for replacing crinoids, chert is absent from the matrix.

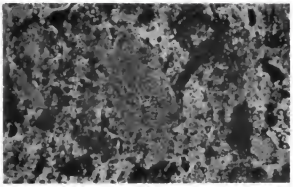

1

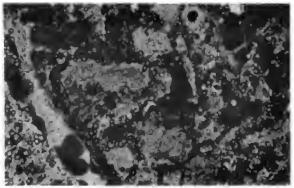

2

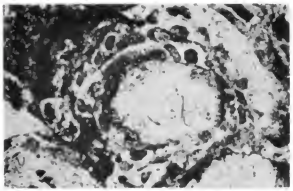

3

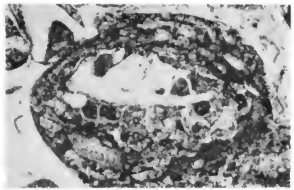

4

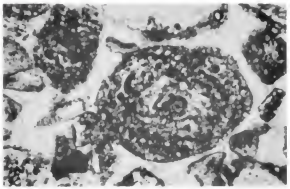

5

6

CHERT/DOLOMITE, *"OSAGIA"* GRAINSTONE, ARGILLACEOUS LIMESTONE

PLATE 11

FIGURE 1. Barite, subsurface, ×33. Euhedral prisms of barite (b) developed as intergranular cement in pellet grainstone.

2. Celestite, subsurface, ×33 crossed nicols. Poikilotopic celestite (white) occupying the intergranular pore space of a pellet grainstone. The dark intergranular space is void.

3. Macrodolomite, 70A–5, +1,880 feet, ×33. Zoned dolomite rhombs and poikilotopic polycrystalline quartz (center). The external morphology of the quartz is analogous to that of the original anhydrite nodule.

4. Anhydrite, subsurface, ×33. Anhydrite nodule (set in microdolomite) with curvilinear orientation of individual laths.

5. Laminated dolomite, subsurface. Nodules in laminated dolomite. These nodules probably were originally composed of anhydrite and formed prior to lithification. They are lined with a 1-mm layer of "cherty" silica and later filled with sparry calcite cement. The sparry calcite does not completely fill the nodule space, and preservation of good crystal terminations on the calcite suggests that the nodule was at one time a void subsequently infilled by both silica and calcite. A large stylolite transects the sample. The laminations are probably of algal origin (algal mats) and, together with the "anhydrite" nodules, a product of sabkha sedimentation.

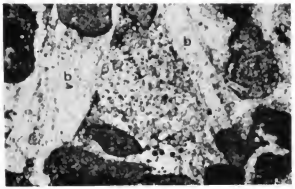

1

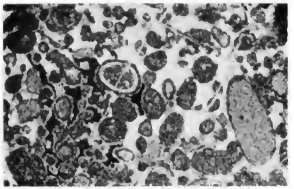

2

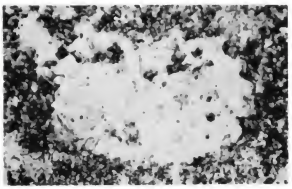

3

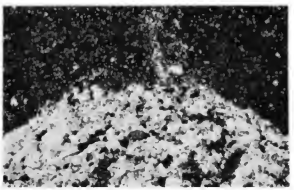

4

5

BARITE, CELESTITE, MACRODOLOMITE, ANHYDRITE, LAMINATED DOLOMITE

PLATE 12

FIGURE 1. Stylolites, 69A–4, 285 feet, ×65. Network of bitumen-filled stylolites, each of which tends to follow the outlines of the crinoid debris. Dolomite rhombs are concentrated along the stylolites.

2. Stylolite, 68A–4B, +20 feet, ×65. Bitumen-filled stylolite in pellet packstone. Anhedral dolomite is present within the stylolite but absent from the adjacent host rock.

3. Bioclastic packstone, 69A–1, base of Kayak Shale, ×65. Sparry-calcite-filled fracture, F, (subvertical) displaced by a later stylolite, S, zone (vertical). The pelecypod clast (right) is preserved in sparry calcite with a radial drusy fabric at its margins passing into an equant fabric. This fabric almost certainly formed by the infilling of a cast by sparry calcite cement.

4. Fractures, 68A–4B, +160 feet, ×33. Parallel hairline fractures filled with sparry calcite cement in a bioclastic pellet wackestone.

5. Bryozoan grainstone, 70A–5, 2,010 feet, ×200. The quartz crystal with well-developed prismatic sides and a tendency to pyramidal termination occurs within a bryozoan fragment. No detrital core is apparent to this crystal, which is probably authigenic.

6. Argillaceous wackestone, 70A–4, 190 feet, ×33. Subparallel lamination of the matrix tends to be interrupted by larger bioclasts. Probably sheared.

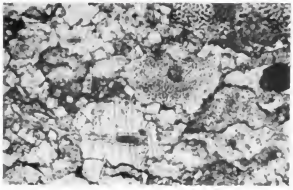

1

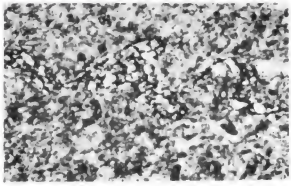

2

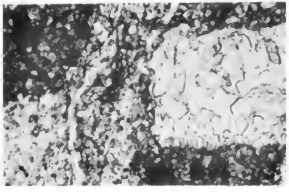

3

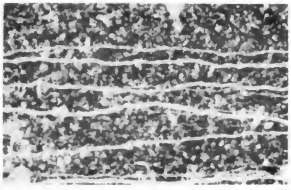

4

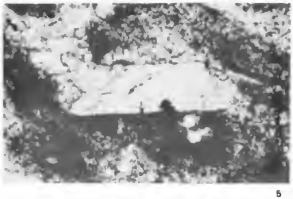

5

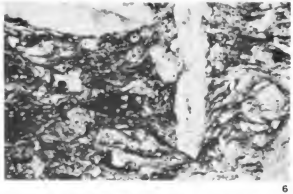

6

STYLOLITES, BIOCLASTIC PACKSTONE, FRACTURES, BRYOZOAN GRAINSTONE, ARGILLACEOUS WACKESTONE